NTNU
Norwegian University of
Science and Technology

Using high resolution horizontal resistivity measurements to estimate resistivity anisotropy, and thus indicate the presence of thin beds in hydrocarbon reservoirs

Fernando Angel

Master's Thesis
Submission date: June 2017
Supervisor: Erik Skogen, IGP

Norwegian University of Science and Technology
Department of Geoscience and Petroleum

First of all, I want to thank the department of Geoscience and Petroleum from NTNU and my supervisor Erik Skogen for giving me the opportunity of researching in this topic and helping me with all the questions I have had, as well as my Master Thesis Tutor at my home university, Domingo Martin Sanchez, from ETSI de minas y energa de Madrid, UPM.

Thanks to NTN-NPD-DISKOS, where I have got all the information about the wells. DISKOS is a national data repository for oil exploration and production related data that is shared by both Authorities and oil companies represented on the Norwegian continental shelf.

Last but not less important, I want to thank my parents, Vicente Angel and Isabel San Jose, and my sister Clara Angel, for all the help they gave me during my educational years.

Abstract

Most commonly used resistivity tools for well logging measure the horizontal resistivity of the formation. A problem appears when you want to measure the true resistivity in a sand reservoir which also contains multiple thin layers of shale. When the layer thickness is below the tools vertical resolution, the thin shale layers make the measured resistivity value lower than the actual resistivity value of the hydrocarbon-saturated sands. As a result, the calculated water saturation is higher than the real value, and the estimation of the volume of oil is lower than the real volume. The resistivity of the sand can be calculated if the vertical resistivity is measured too, and this can be done with a triaxial induction tool, however, this is rarely done due to the additional cost.

The objective of this project is to investigate methods to estimate the vertical resistivity from the horizontal resistivity in the absence of triaxial measurements. The work began by reviewing the published literature related to this topic, and identifying some methods that achieved something similar. The paper from Tabanou et al. (2002) was used as a reference for the development of one of the methods; estimating Rv using a convolution average filter.

Three algorithms were programmed and tested with resistivity data from six different wells, half of them water based mud, and the other half oil based mud. The results were satisfactory, not finding a general method that works in every case, but concluding that if the method chosen is the best option for the well and formation conditions, a high probability of success is achieved.

Table of Contents

List of Tables

List of Figures

Abbreviations

AIT	=	Array Induction tool.
$AORX$	=	Array Induction shadow resistivity.
$AT10$	=	Array Induction 10” resistivity.
$AT90$	=	Array Induction 90” resistivity.
GR_{max}	=	Gamma ray value of the sand.
GR_{min}	=	Gamma ray value of the shale.
$HRLT$	=	High Resolution Laterolog Array Tool.
l_n	=	Length (thickness) of the thin layer.
L	=	Total length of the window for R_v and R_h.
NTG	=	Net to gross ratio.
OBM	=	Oil based mud.
$OBMI$	=	OBM resistivity microimage tool.
R_s	=	Resistivity of the sand.
R_{sh}	=	Resistivity of the shale.
R_t	=	Resistivity of the formation.
R_v	=	Vertical resistivity.
R_h	=	Horizontal resistivity.
A	=	Resistivity anisotropy (ratio of R_v/R_h) .
$RXOI$	=	Invaded zone formation resistivity very high resolution.
V_s	=	The volume of sand over 1 (sand fraction).
V_{sh}	=	The volume of shale over 1 (shale fraction).
WBM	=	Water based mud.

Chapter 1

Introduction

Whereas in the past the search for commercial hydrocarbon accumulations in siliciclastic rocks typically involved identification of thick, clean, i.e. shale-free sands, it is now increasingly more focus on the evaluation of the reservoir potential also of shaly sands formations. However, the well log evaluation of this type of reservoirs is more complicated than that of the clean sands due to the presence of shale in the reservoir, and the evaluation is even more complicated if the reservoir is formed with thin layers of sand alternating with thin layers of shale. Thin layers here refer to those that have a thickness which is below the resolutions of conventional logging tools, typically on the order of 30-50 cm. The presence of thin layers are relatively common because a big number of turbiditic offshore reservoirs are thinly laminated.

Fig. 1.1 shows an example of this type of formation with a 1m core exposed to ultraviolet light that makes the hydrocarbons-bearing sands light up whereas the thin shale laminations remain dark.

Figure 1.1: 1m of a core sample seen in ultraviolet light.

The presence of thin beds represents one of the most common problems in a shaly sand interpretation because it makes it difficult to determine effective porosity, true resistivity and, by extension, water saturation and permeability. The problem with the porosity and resistivity tools is that they have vertical resolutions from 0.3m to 2.5m, so they can not measure the true properties of thin layers as they are strongly affected by the adjacent layers.

Most commonly used resistivity tools for well logging measure the resistivity perpendicular to the wellbore, this will be the horizontal resistivity if the well is drilled perpendicular to the formation layers. A problem with these tools appears when you want to measure

the true resistivity in an anisotropic reservoir which consists of multiple thin layers of sand and shale (laminated sand-shale reservoirs). Thin shale layers make the measured resistivity value, typically horizontal resisivity (R_h), lower than the actual resistivity value in the hydrocarbon-saturated sands. As a result, the calculated water saturation is higher than the real value, and the calculated Oil-In-Place is lower than the actual volume. One way of solving this problem is to measure the vertical and the horizontal resistivity with a Triaxial Induction tool, however, this is rarely done due to the added cost.

The objective of this project is to investigate methods to determine relationships between the vertical and horizontal resistivities in order to obtain the true sand resistivity in the thinly bedded formation.

Because of the importance of these type of reservoirs, it is necessary to find a way of doing a correct petrophysical evaluation, finding the relationship between the electrical anisotropy and the response of different electrical tools. **Fig. 1.2** shows the theoretical resistivity model of a thin laminated reservoir, where Rt is the real resistivity of the formation, representing the resistivity of the hydrocarbon-saturated sand in the highest points, and the shale resistivity in the lowest points, and the horizontal (Rh) and vertical (Rv) resistivities as measured by a resistivity tool with limited thin bed resolution.

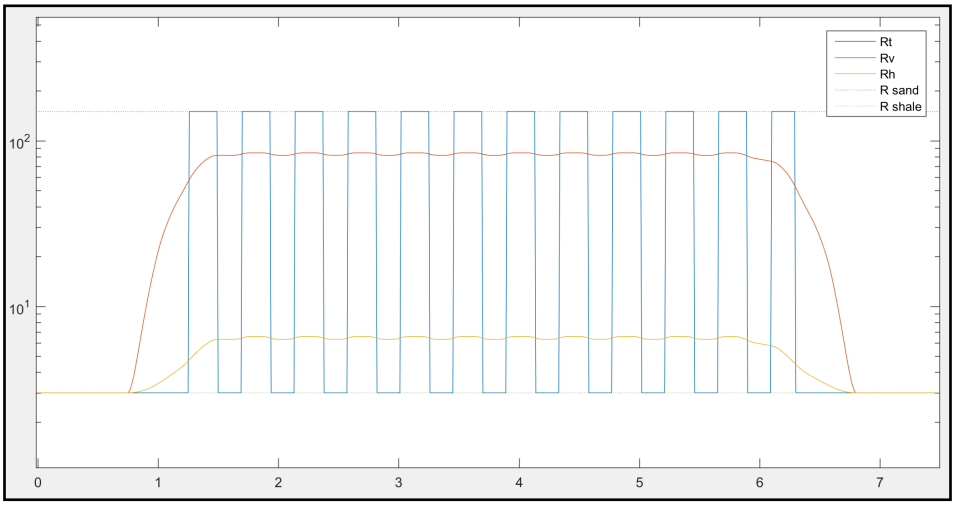

Figure 1.2: Theoretical resistivity model of a thin laminated reservoir. X axis in m and Y axis in ohm.m.

As it is shown in **Fig. 1.2**, the underestimation of resistivity in the sands (R_h vs R_{sand}) introduces a large error in a thin laminated reservoir. Because of that, finding a way of calculating the real R_{sand} becomes very important.

This Master Thesis has used well logging data from 6 successful exploration wells drilled in the Barents Sea and the Norwegian Sea after year 2000. The data base has been supplied by NTN-NPD-DISKOS. Diskos is a national data repository for oil exploration and production related data that is shared by both Authorities and oil companies represented on the Norwegian continental shelf. **Fig. 1.3** shows the localization of the well studied.

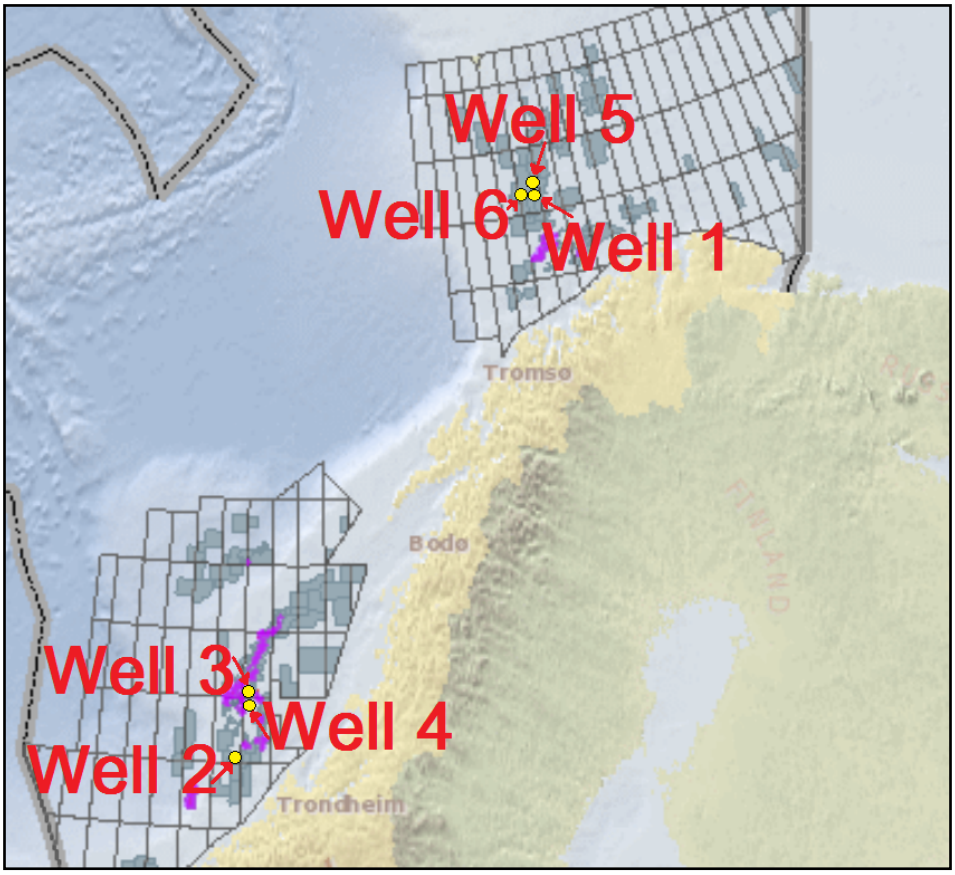

Figure 1.3: Locations of the wells studied. Wells 1, 5 and 6 in the Barents Sea, wells 2, 3 and 4 in the Norwegian Sea.

The data supplied by Diskos, the DLIS files, has been processed in Techlog software in order to plot the logs that are shown in appendix A, and in order to export the files in csv format. Techlog has been used for helping in the petrophysical interpretation and selecting the best resistivity curves for applying the algorithm. The data have been converted to csv format for being able to be read by Matlab, the software that has been used for programming the algorithms.

Chapter 2

Literature Review

2.1 Passey et al. (2004)

The publication of Passey et al. (2004) explain two methods that try to solve the problems with the reservoirs with thin beds that are less thick that the vertical resolution of conventional logs. This cause a big effect in the resistivity measurements, usually, underestimating hydrocarbon volume by 30% or more.

The systematic approach to evaluate hydrocarbons in place from a thin laminated reservoir is divided in two methods; high-resolution method and low-resolution method, the first one is applied to thin layers thicker than 0.3m, the second can be applied to all types, but it is useful when layers are thinner than 0.3m.

The high resolution method consists of using very high resolution tool (image log or density log) for defining boundaries of each layer. Then, an estimation of properties of each layer have to be entered as an input, and an algorithm will calculate the log response for these input parameters. The log response will be compared with the real log response and parameters will be changed until the error between the estimated and real log responses will be minimum.

The low resolution method does not attempt to solve individual beds, it consist on building a statistical earth model with different alternatives of bed thickness and petrophysical properties. Then, an algorithm will predict the average log response with these input values, and a Monte Carlo inversion method will find the ranges of bed properties and frequencies that match better the real log response, obtaining an estimation of the uncertainty too.

These methods have been used around the world and, in many cases, the output earth model has been compared with core based assessments having positives results, increasing the hydrocarbon volume in thin bed reservoirs. These methods are being applied by ExxonMobil for evaluating their oil and gas reservoir. With the correct input data and accurate algorithms, these methods can be very useful.

2.2 Tabanou et al. (2002)

The publication of Tabanou et al. (2002) was written more or less at the same time that Triaxial Induction tool was invented and resistivity-imaging tool for oil base mud (OBMI) was introduced in the industry. The article tries to find the benefits and limitations of analyzing thinly laminated reservoirs with high resolution sensors in a well drilled with oil based mud.

The high resolution method consists in applying to the OBMI (micro-)resistivity log two average convolution filters, based on equations (2.1) and (2.2), with a length of the window of 0.6 meters, for computing Rv and Rh.

$$R_v(z) = \int_{\frac{-H}{2}}^{\frac{H}{2}} R_{obmi}(z') \cdot F_h(z - z') \cdot dz' \tag{2.1}$$

$$\frac{1}{R_h(z)} = \int_{\frac{-H}{2}}^{\frac{H}{2}} \frac{F_h(z - z')}{R_{obmi}(z')} \cdot dz' \tag{2.2}$$

The results are quite satisfactory if the invasion is not very deep and the thin layers are thicker than 15 cm, if they are thinner, results will gradually be less reliable until layers of 1.5 cm, which is considered the limit for using this method with an OBMI tool. It is important to know that this method measures only the anisotropy due to interspersion of high resistivity layers with low resistivity layers, this method can not be applied to compute intrinsic anisotropy within a layer. If the reservoir has carbonate streaks, these will overestimate the cumulative oil volume due to the high increase of the resistivity on these streaks, but if they are thick enough to be identified by OBMI, the high resistivity peaks can be removed with an algorithm for getting the real values of the anisotropy.

The method used in Tabanou et al. (2002) worked very well on a small scale in an OBM well, an objective of the present thesis will be try to do something similar in a WBM well, and using that method in a bigger scale, instead of using half meter filter, using a bigger window for trying to identify anisotropic zones along all the well.

2.3 Woodhouse et al. (1984)

The publication of Woodhouse et al. (1984) is the development of a deconvolution filter that tries to reduce the bed effect on the deep induction log of wells that are deviated less than 30^o. This filter works with logs with a vertical resolution of 0.3m or less, and with beds ticker than 1.2m. It can not be applied where low-resistivity conditions (3 ohm.m) exist, due to the skin effect that complicate the response.

Initially, the induction log data were converted to the frequency domain spectrum using a Fourier transform, then, it was smoothed using a polynomial curve-fitting technique. Next, comparing it with the sonic log, a filter was applied for emphasizing the high frequency response of the induction log. This result was compared with the deep and shallow laterologs response, and that showed that the initial deconvolution filter introduced oscillations that were not present in laterolog curves and they were not expected to be there. The initial filter was empirically modified for matching the laterolog response, obtaining the final deconvolution filter that is shown in **Fig. 2.1**

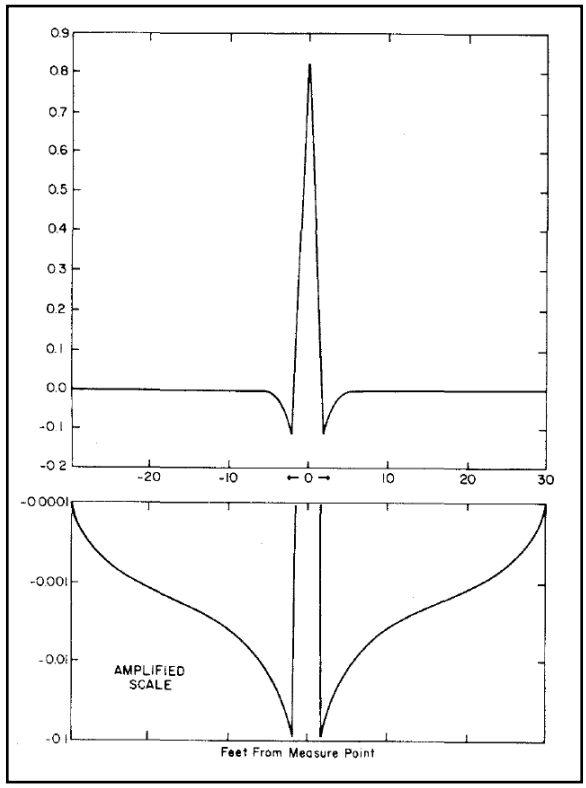

Figure 2.1: Deconvolution filter applied in Woodhouse et al. (1984).X axis in feet and Y axis in ohm.m.

This paper was one of the first that proved that the induction response can be improved by software signal processing for obtaining a better curve in a thin bed laminated reservoir.

Chapter 3

Methodology

Wells 1, 5 and 6 are water based mud wells, and wells 2, 3 and 4 are oil based mud wells. Wells where Triaxial Induction Tool was available were preferred, however, this tool has not been used in most wells, and most of the wells where it has been used are water based mud wells. Therefore, and extra oil based mud well without Triaxial Induction tool has been used, well number 2.

In all the thesis, the way chosen for measuring the depth is the measured depth (MD), which is the length along the wellbore path.

In the section 3.1 of this chapter the problem of thin laminated reservoir has been solved in the case that Triaxial Induction tool was available. The purpose of this section is to show how different is the resistivity of the sand, calculated with this tool, and the horizontal resistivity, as measured by conventional (uni-axial) resistivity tools. As it has been said before, Trixial Induction tool is not commonly used because of the added cost, so the rest of the sections of this chapter explain how Rv and Rh can be estimated from three different methods, all using algorithms that use the horizontal resistivity as input data.

3.1 Calculating the resistivity of the sand from the Triaxial induction tool

The Triaxial Induction tool provides 3D information about the formation resistivity using a transmitter in the directions of x, y and z, and a receiver which reads the signals in the same directions. From the matrix 3X3 that we get as a result, Rv and Rh can be calculated, knowing that Rv is the resistivity in the perpendicular direction to the layers, and Rh is the resistivity in the same directions that the layers.

The vertical resistivity could be represented as the averaged sum of the resistivity of each layer, representing the layers as resistivities in series mode:

$$R_v = \frac{\sum_{n=1}^{n} \cdot L_n \cdot R_t}{L} \tag{3.1}$$

If we want to calculate the horizontal resistivity, the average sum of the resistivity of each layer may be done representing layers as resistivities in parallel mode:

$$\frac{L}{R_h} = \sum_{n=1}^{n} \frac{L_n}{R_t} \tag{3.2}$$

The well that we are going to use in this demonstration is well 1. This well is drilled with water based mud and the anisotropy has been calculated along all the well. The interpretation of this well is straightforward since Rv and Rh have been calculated from the Triaxial Induction tool.

Fig. 3.1 is a representation of the anisotropy (ratio between Rv and Rh), shown in equation (3.3), along 1000m of the well, the hydrocarbon bearing reservoir being located from 1276 to 1395 m. We can see that there are several zones with anisotropies that are higher than 4, it is not easy to find the thinly laminated intervals because the pure shale is highly anisotropic too, however, we can see a less spiky interval with high anisotropy around 1375m.

$$A = \frac{R_v}{R_h} \tag{3.3}$$

For differencing shale anisotropy from the thin laminated reservoirs we can use the gamma ray log in **Fig. 3.2**, where we can see that the other high anisotropy zones have a huge GR value.

In the zone of interest, knowing Rv and Rh, we can calculate the resistivity of the sand if we estimate the volume of shale of each point. The easiest way of solving the Vsh is using GR tool, as it is shown in the next equations.

$$V_{sh} = \frac{GR - GR_{min}}{GR_{max} - GR_{min}} \tag{3.4}$$

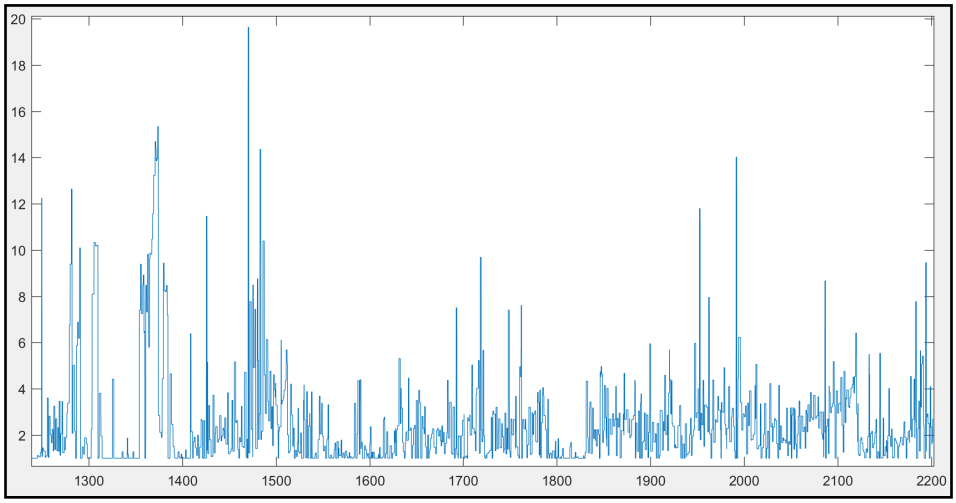

Figure 3.1: Anisotropy along the well. X axis in m and Y axis is the ratio of R_v/R_h.

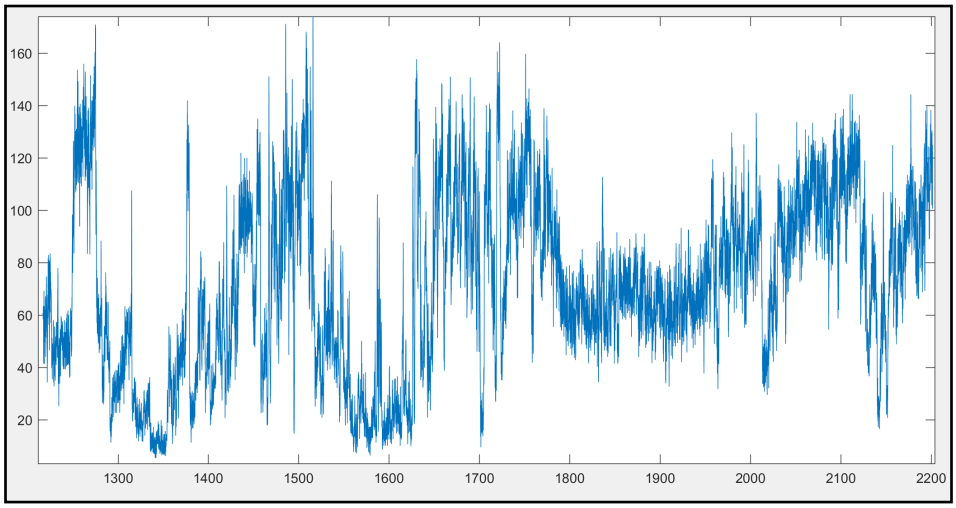

Figure 3.2: Gamma ray log. X axis in m and Y axis in GAPI.

$$V_s = 1 - V_{sh} \tag{3.5}$$

$$\frac{1}{R_h} = \frac{V_s}{R_s} + \frac{V_{sh}}{R_{sh}} \tag{3.6}$$

$$R_v = V_s \cdot R_s + V_{sh} \cdot R_{sh} \tag{3.7}$$

Solving the equation system, we obtain that the resistivity of the sand is a quadratic equation where we have to get the positive value.

$$R_s^2 \cdot (R_h \cdot V_s) + R_s \cdot (V_{sh}^2 + R_h \cdot V_s - R_h \cdot R_v) + V_s \cdot R_s = 0 \tag{3.8}$$

Solving the problem of the well with the equations mentioned before, we get the resistivity for the hydrocarbon bearing sand shown on **Fig. 3.3**.

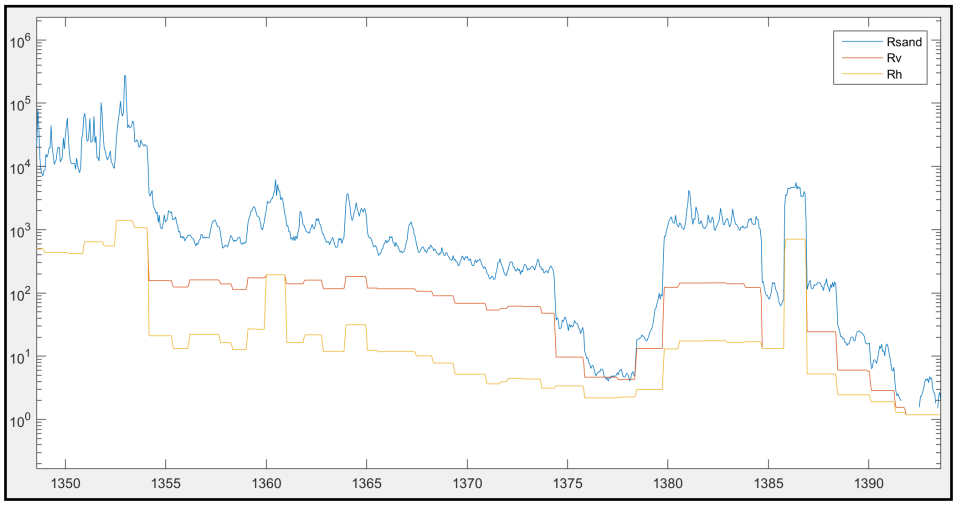

Figure 3.3: Resistivity of the sand in the interesting zone. X axis in m and Y axis in ohm.m.

With the resistivity of the sand, if we know the porosity from another tool, and we know the resistivity of the formation water, we can calculate the saturation of water from Archie equation, which will let us knowing the real oil saturation from the thin laminated reservoir.

This example demonstrates clearly how the horizontal resistivity alone will lead to an underestimation of hydrocarbon saturations, and how R_{sand} calculated from R_h and R_v will give a more accurate result.

3.2 Method 1: estimating Rv from a convolution average filter.

The algorithm created (appendix B) is based on the article of Tabanou et al. (2002), however, it has been tried to make it works in more types of wells. The algorithm needs the inputs of resistivities, depths, and the length of the window that it is going to be used for averaging each value. The window length depends on the resolution of the log, a very high resolution log will need between 5m and 10m, but a normal log will need window lengths between 20m and 50m for getting satisfactory results. Another important criteria is that total reservoir interval has to be ticker than the window length for reaching the real value of the anisotropy. What the algorithm does is calculating the average resistivity for each depth, from minus half distance of the window length until plus half distance of the windows length.

There are three outputs from this algorithm, one is Rv, which is calculated with the equation (3.1), Rh, which is calculated with equation (3.2), and the anisotropy, A, which is the ratio of Rv over Rh.

A theoretical thin laminated reservoir has being created with the resistivities values of 150 ohm.m in sand with gas, 20 ohm.m in the sand with oil and 3 ohm.m in the shale. The objective is analysing how the algorithm works and what are the boundary effects that we should take into account. **Fig. 3.4** and **Fig. 3.5** show the results of applying the algorithm with a window length of 60m. **Fig. 3.4** with a NTG of 50%, where half of the reservoir is hydrocarbon saturated sand and the other half is shale, and **Fig. 3.5** with a NTG of 10%, where 90% of the reservoir is shale. It has been seen that, if the NTG is less than 50%, the boundary effect does not have any peak and anisotropy can be read when the line is stabilized, however, if the NTG is more than 50%, the boundary effect will make peaks in the contacts between shale and reservoir and between sand saturated in water and sand saturated in hydrocarbons. The peaks will have a higher value that the real anisotropy and it is important to use a length of windows short enough for reaching stable zones of the anisotropy for doing a proper calculation.

These models have been done with different NTG rates for getting the relationship between the anisotropy and percentage of shale. The results are shown on **Fig. 3.6**, where it is shown that the maximum value of anisotropy is with a NTG of 50%, and the distribution is quite similar in oil and gas.

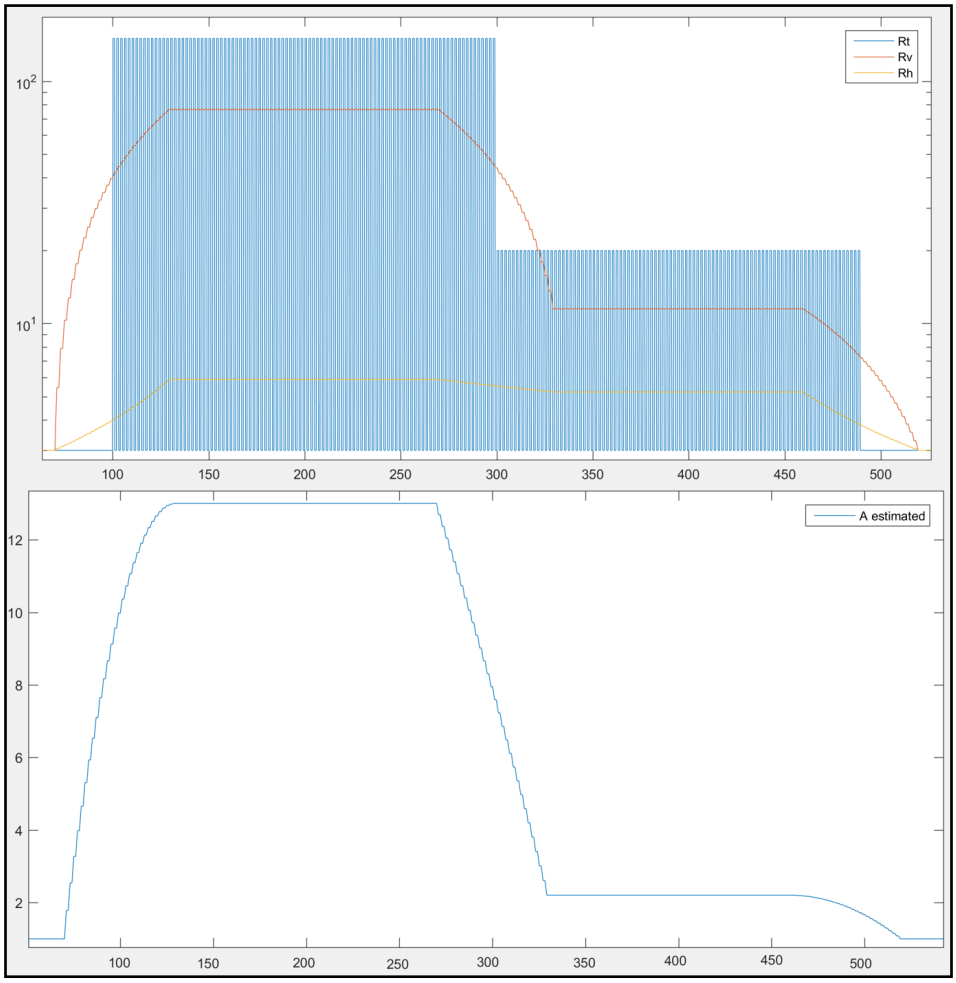

Figure 3.4: Theoretical reservoir with a NTG of 50%. X axis in m and Y axis in ohm.m for resistivity and the ratio of R_v/R_h for the anisotropy.

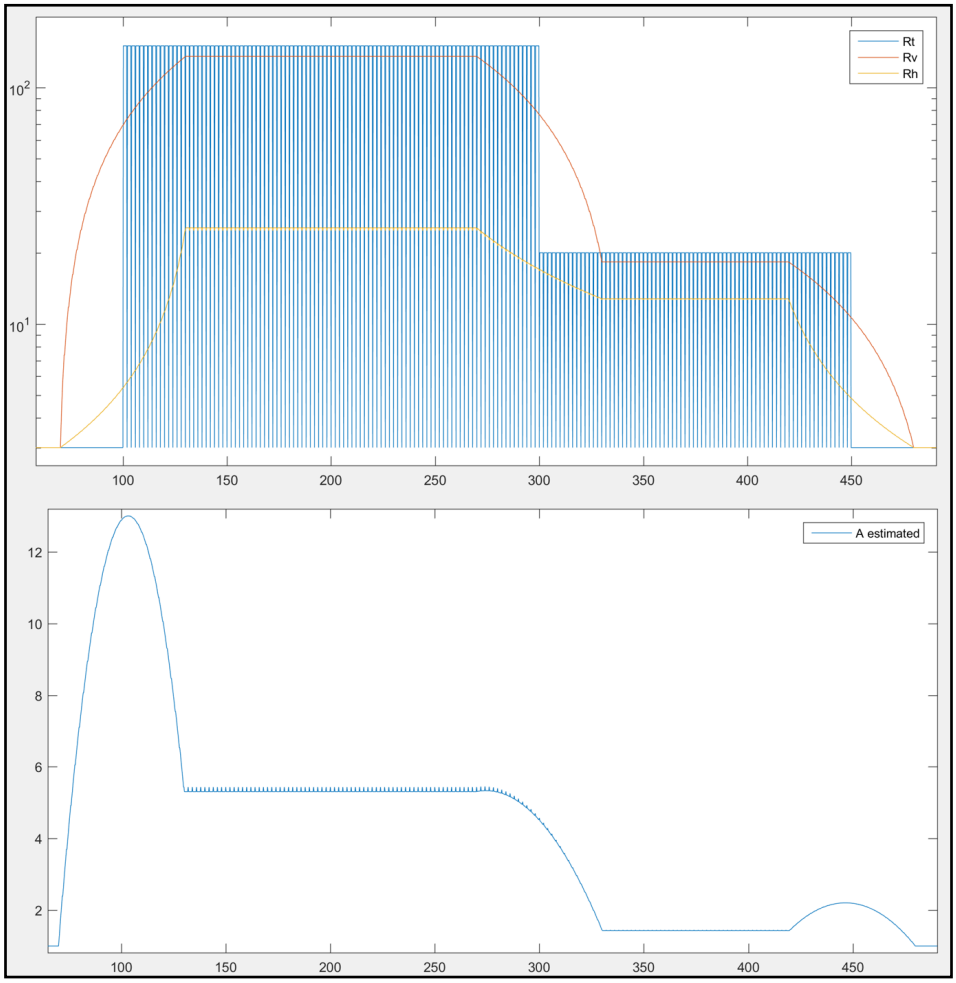

Figure 3.5: Theoretical reservoir with a NTG of 10%. X axis in m and Y axis in ohm.m for resistivity and the ratio of R_v/R_h for the anisotropy.

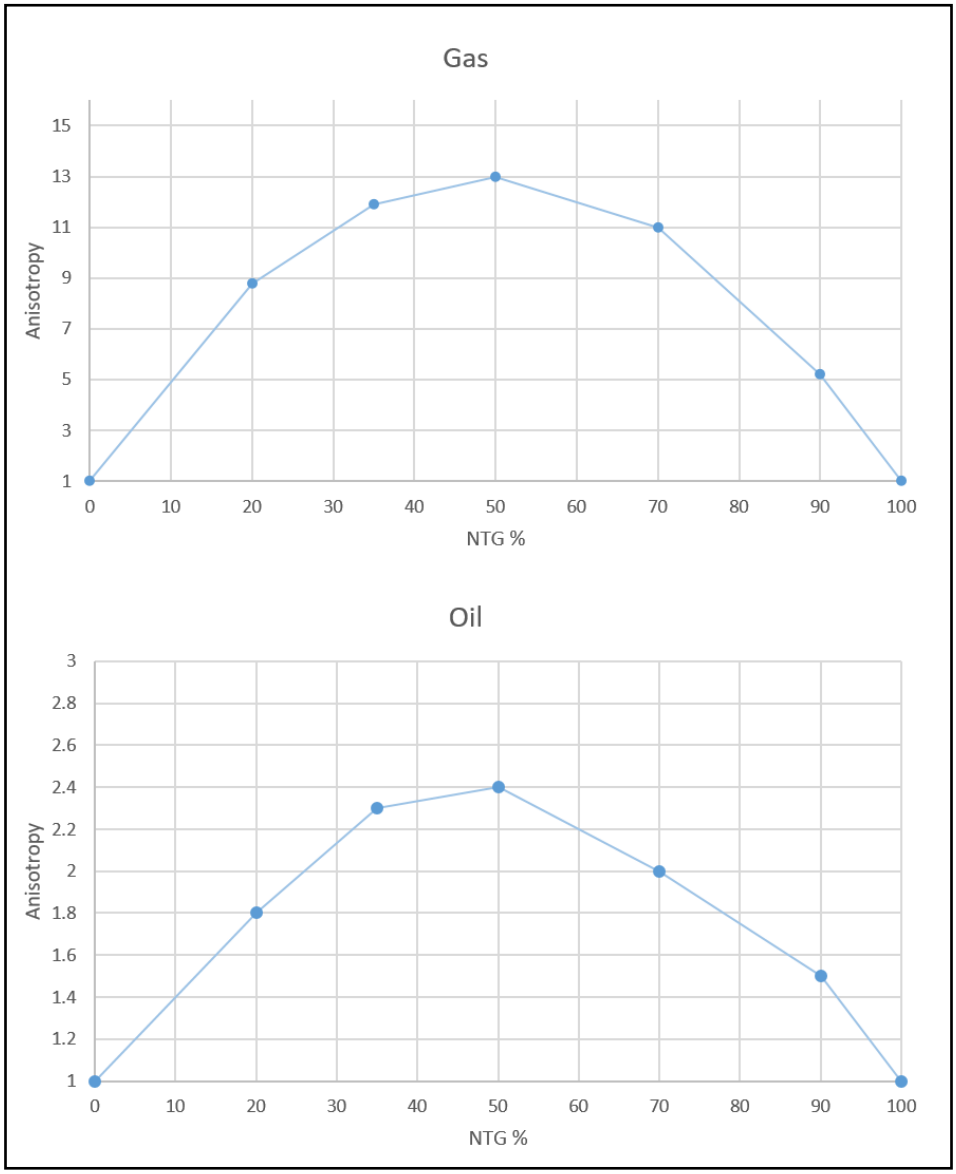

Figure 3.6: Relationship between anisotropy and NTG. X axis in % and Y axis is the ratio of R_v/R_h.

3.3 Method 2: estimating Rv from the estimation of the resistivity of the sand.

The algorithm in method 2 (appendix B) consists of estimating Rs and Rsh from high resolution resistivity logs and thereby being able to compute Rv and Rh. The basis for this is that, in a very high resolution resistivity log in a thinly laminated reservoir, the signal will be very spiky because of the high resistivity of the oil saturated layers and the low resistivity of the layers of shale. Therefore, if we are able to obtain these resistivities from the regular resistivity log, we will get Rs and Rsh and the calculation of Rv will be trivial.

For computing Rs, we analyse the resistivity measured by a high resolution resistivity tool during a window length that we have introduced as an input (normally between 1 and 2 meters). The maximum value during that window will be set as the Rs for that windows length and the Rsh can be set as a constant, measured in a nearby thicker shale. It has been tried to compute Rsh as Rs, with the minimum value of the window length, however, the results has been bad because of the relatively low resolution of the tool.

Knowing this, we only need the Vsh and Vs, this can be calculated using Gamma Ray tool and applying equations (3.4) and (3.5). Introducing all these data in equations (3.6) and (3.7) we are able to compute Rv and Rh, as it is shown on **Fig. 3.7**

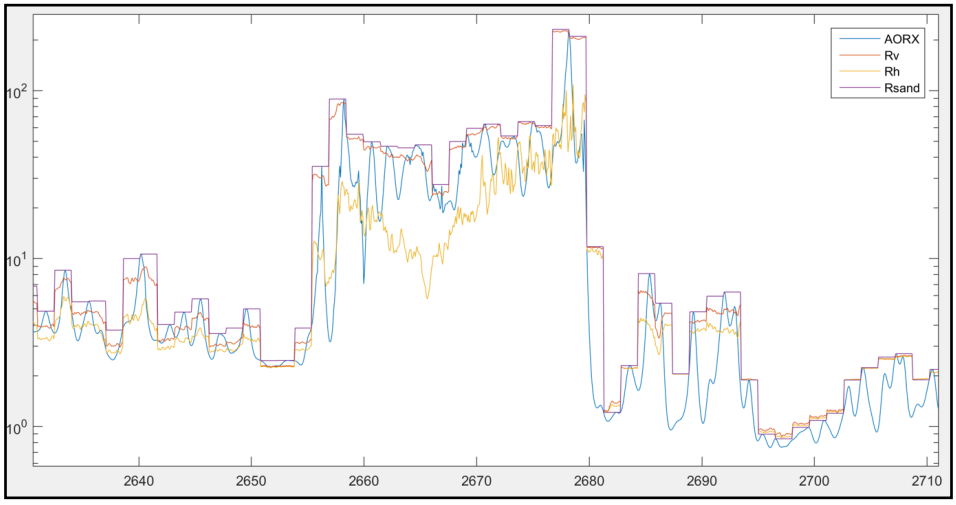

Figure 3.7: Rv and Rh calculation example from AORX, estimating R_s. X axis in m and Y axis in ohm.m.

3.4 Method 3: estimating Rv from the deep resistivity and GR tool.

The only resistivity tool that can identify thin layers is RXOI or OBMI, the problem with these tools in a water based mud is that they read the resistivity values in shales and in the water invaded zone of sands, so these values are not very useful.

The way of solving this problem with an algorithm (appendix B) is using equations (3.4) and (3.5) for getting the volume of shale and volume of sand from GR tool, and using equations (3.6) and (3.7) for calculating the vertical resistivity. For solving this equations we need to estimate the horizontal resistivity as Rt from HRLT or AT90, and we need to measure the resistivity of the shale. The way chosen for getting the resistivity of the shale is reading it in a pure shale area, as it is shown on **Fig. 3.8**. We can see that the resistivity of the shale is between 2 and 4 ohm.m.

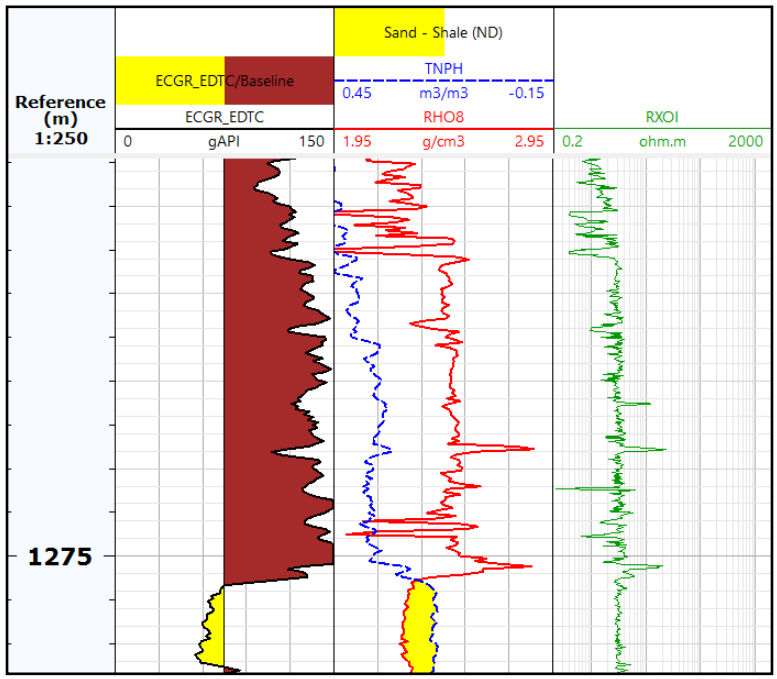

Figure 3.8: Pure shale where the resistivity of the shale can be read in the RXOI log.

Using all data mentioned before as an input, and and an adequate window length for smoothing the signal, it is possible to calculate the vertical resistivity and, therefore, the anisotropy.

Chapter 4

Results

Table. 4.1 shows some details of the wells studied. Well logs from these wells can be seen in appendix A.

	Well 1	Well 2	Well 3	Well 4	Well 5	Well 6
Mud type	WBM	OBM	OBM	OBM	WBM	WBM
Maximum deviation (°)	3.20	33.00	15.10	10.60	4.46	6.00
Interval available (m)	1000	1700	400	130	800	1150
Top log interval (m)	1250	2300	2600	3765	900	1050
Bottom log interval (m)	2250	4000	3000	3895	1700	2200
Rv and Rh available?	Yes	No	Yes	Yes	Yes	Yes
RXOI available?	Yes	No	No	Yes	Yes	Yes
Gas interval (m)	37	93	11	0	28	47
Oil interval (m)	83	134	14	40	47	128

Table 4.1: Summary of the wells

4.1 Method 1: estimating Rv from a convolution average filter.

4.1.1 Well 1

Convolution filters are used for smoothing signals that are very spiky. The most basic convolution filter is an average filter, which gives the same weight to all values of the windows chosen. This algorithm has been explained in chapter 3. **Fig. 4.1** shows the result of this filter over Rt from HRLT of the well 1, which is WBM, using a window length of 15 m.

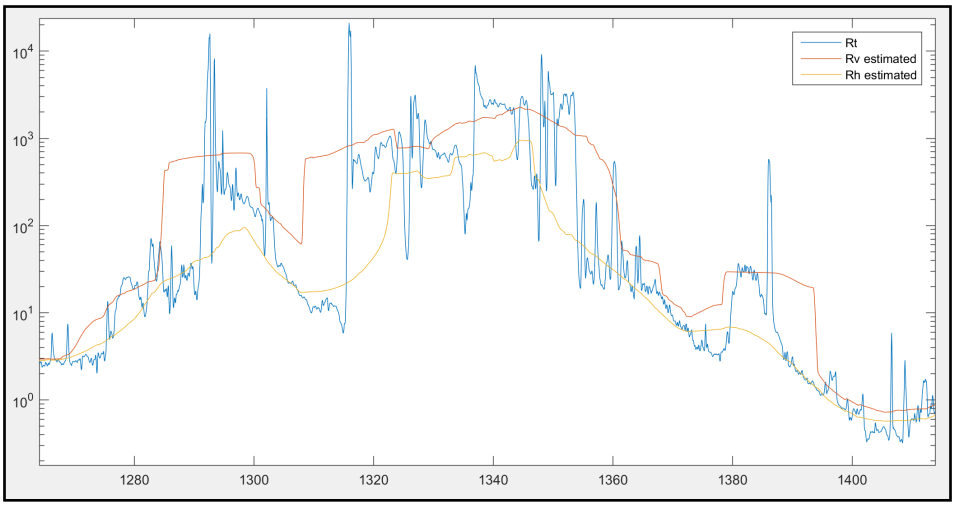

Figure 4.1: Average filter of 15m over Rt from HRLT in well 1. X axis in m and Y axis in ohm.m.

If we compare anisotropies instead of vertical resistivities, we can clearly see where the thinly laminated reservoir is, as it is shown on **Fig. 4.2**. **Fig. 4.3** shows only the zone of the reservoir, where we can see that the reservoir shows anisotropy in some places, but it is less that the Triaxial Induction Tool value (A measured).

If we use a convolution filter with a Gauss distribution we obtain similar results with a more smoothed line, as it is shown on **Fig. 4.4**, which has a window length of 15 m too. The Gauss filter has not been used in the next wells because it has been proven that the results do not improve, for simplification, only linear filter has been applied.

If we use the AT90 log, we get a stable anisotropy of 4 along all the reservoir. This can be seen on **Fig. 4.5**. **Fig. 4.6** shows the same log along all the well, it can be seen that the algorithm is able to identify the thin laminated reservoir.

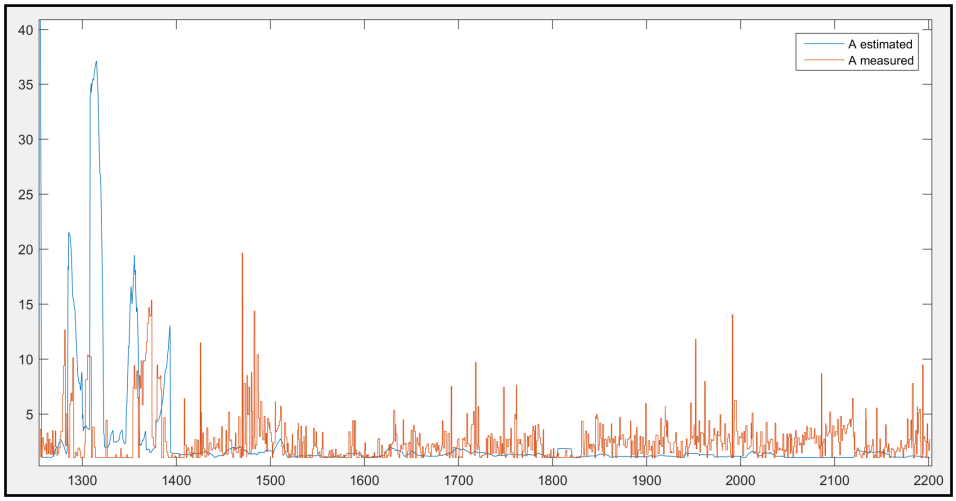

Figure 4.2: Anisotropy estimated with an average filter of 15m over Rt from HRLT in well 1. big scale. X axis in m and Y axis is the ratio of R_v/R_h.

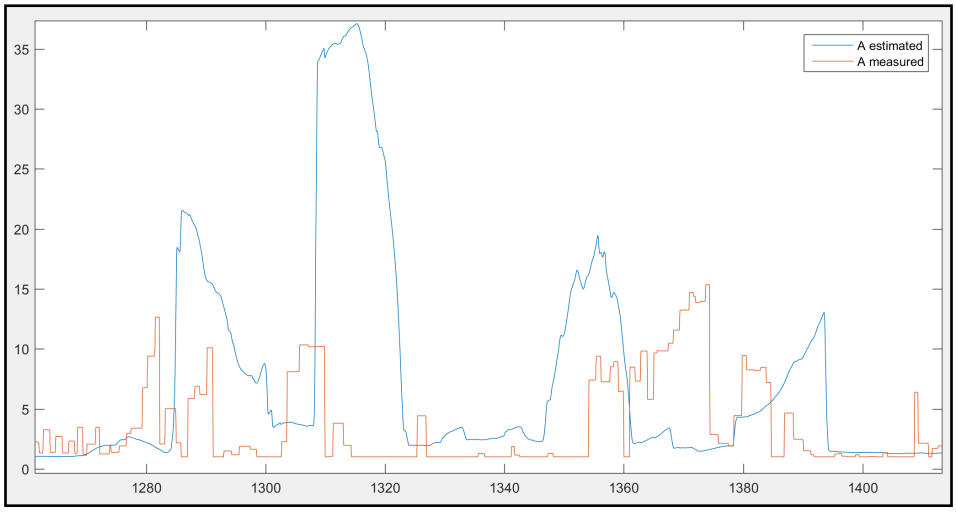

Figure 4.3: Anisotropy estimated with an average filter of 15m over Rt from HRLT in well 1 along the reservoir. X axis in m and Y axis is the ratio of R_v/R_h.

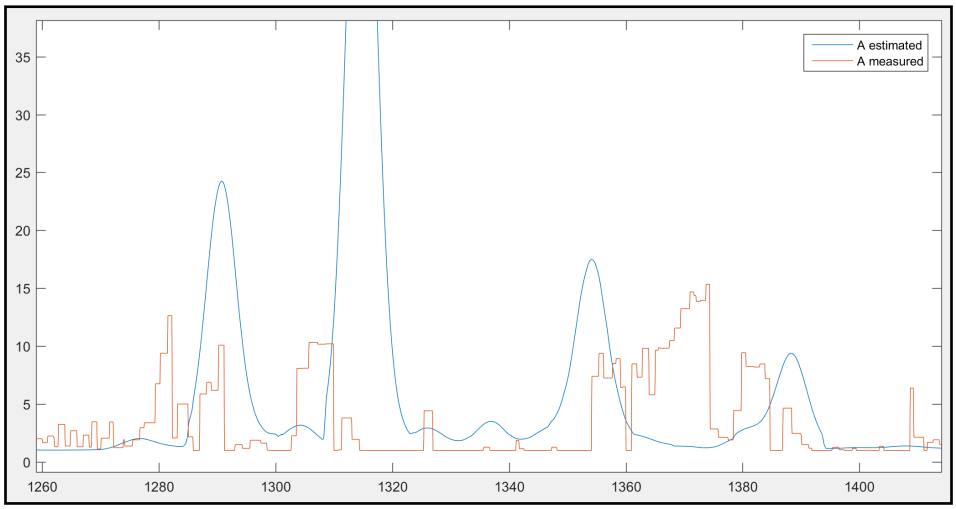

Figure 4.4: Anisotropy estimated with a Gauss filter of 15m over Rt from HRLT in well 1 along the reservoir. X axis in m and Y axis is the ratio of R_v/R_h.

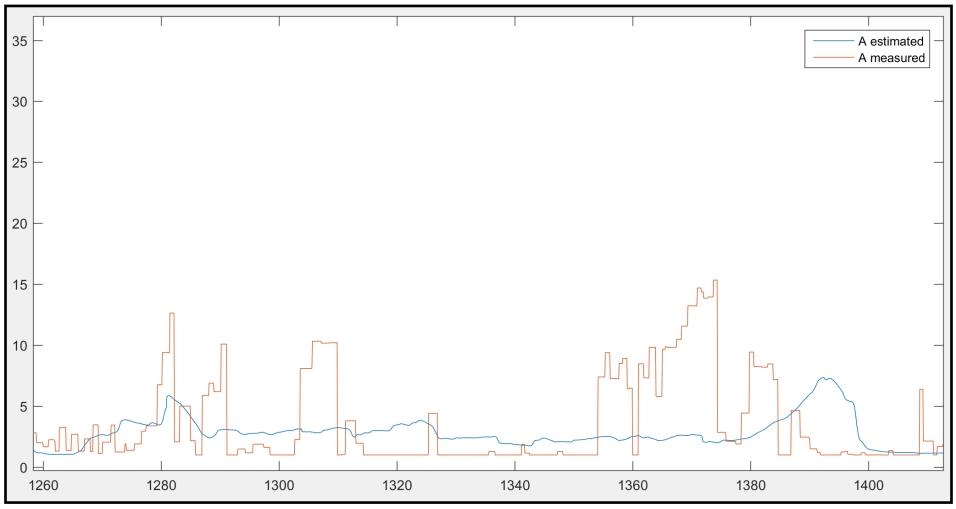

Figure 4.5: Anisotropy estimated with an average filter of 23m over Rt from AT90 in well 1 along the reservoir. X axis in m and Y axis is the ratio of R_v/R_h.

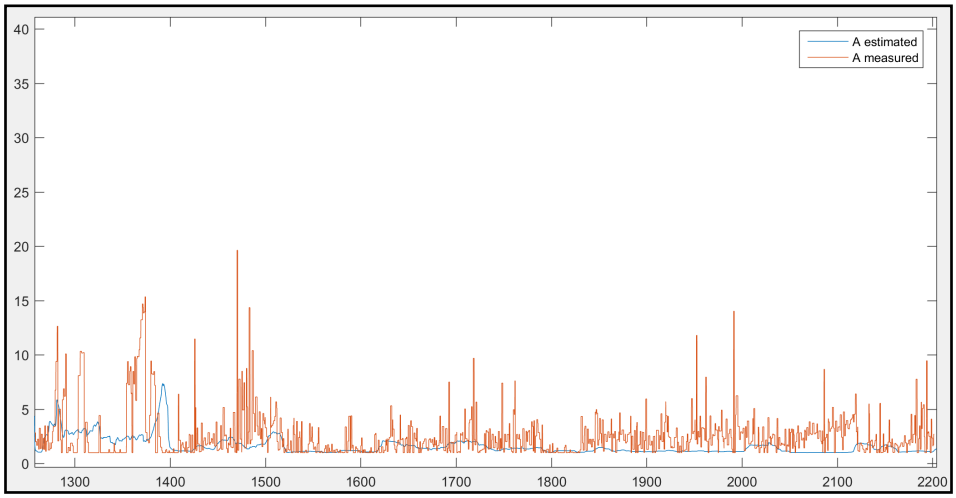

Figure 4.6: Anisotropy estimated with an average filter of 23m over Rt from AT90 in well 1. Big scale. X axis in m and Y axis is the ratio of R_v/R_h.

4.1.2 Well 2

The algorithm has been applied over the well 2, which is OBM, however the triaxial tool was not used in this well, so we can not do a comparison with a measured anisotropy. Applying the average algorithm to the AT90 log (Rt) with a window length of 75m we obtain Rv and Rh, shown on **Fig. 4.7**. **Fig. 4.8** shows the anisotropy estimation.

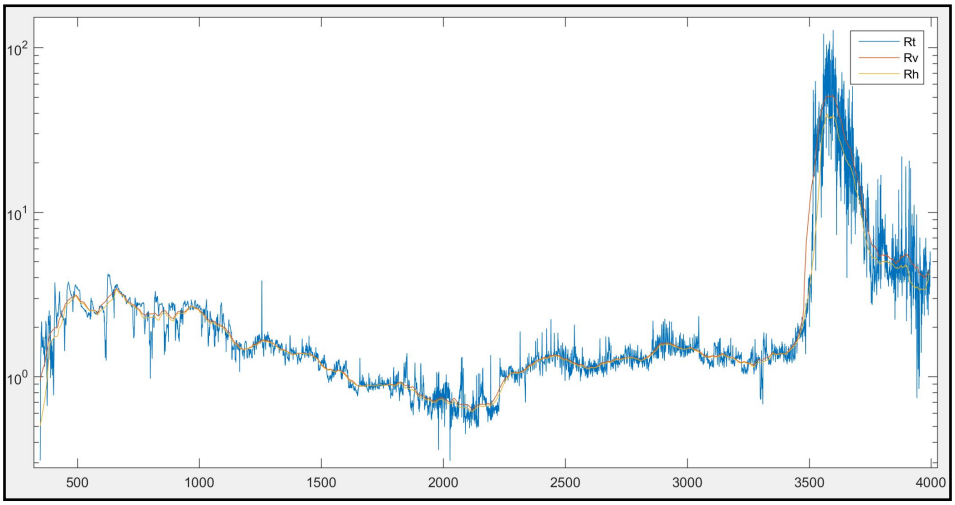

Figure 4.7: Rv and Rh estimation with an average filter of 75m over AT90 of well 2. Big scale. X axis in m and Y axis is in ohm.m.

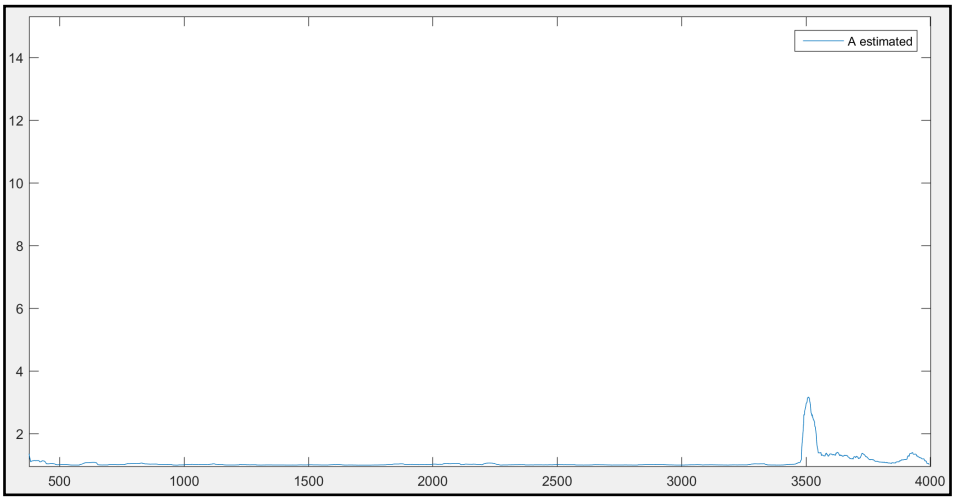

Figure 4.8: Anisotropy estimation with an average filter of 75m over AT90 of well 2. Big scale. X axis in m and Y axis is the ratio of R_v/R_h.

If we analyse the different logs of the well 2, we can see that all the reservoir likely have thin layers of shale because all logs are very spiky. However, these thin layers are not like well 1, there are less number of them and they are thicker, so this is a good example for using the algorithm. Analysing the logs, we can find the top of the reservoir, the GOC and OWC, this can be seen in the anisotropy estimated plot too, if we take into account that the top of the reservoir and the OWC are in the high peaks. The GOC is more difficult to see, but it is expected to be in the change of anisotropies from gas to oil . This is shown on **Fig. 4.9**, where the vertical scale has been increased.

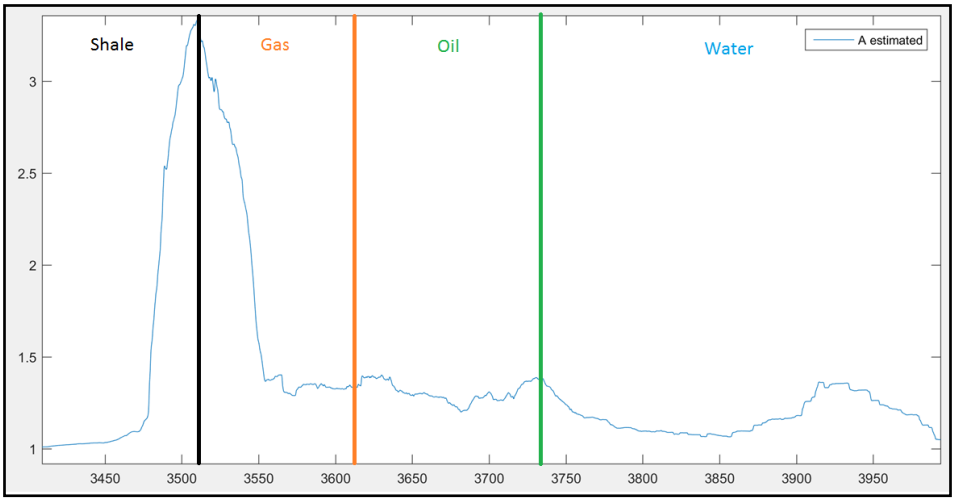

Figure 4.9: Anisotropy estimation with an average filter of 75m over AT90 of well 2, along the reservoir. X axis in m and Y axis is the ratio of R_v/R_h.

We can read that the anisotropy in the gas zone is between 1.3 and 1.4, and in the oil zone is between 1.3 and 1.2. There are two theories for explaining these low values.

The first theory is that the NTG is so high that it does not affect a lot the anisotropy, the other theory is that this algorithm does not show the real anisotropy, it is just an indication of the place where the anisotropy takes place.

4.1.3 Well 3

Well 3 is an OBM well where there is a reservoir of 20m with gas and oil. The algorithm did not show the expected results because the reservoir is very thin, and for being able to read the anisotropy without boundary effect, the window length has to be less than 20m, which is quite low for the low resolution of the resistivity tool used. **Fig. 4.10** shows the estimation of Rv and Rh, and **Fig. 4.11** shows the anisotropy estimation, where the two high peaks are the boundary effects, and the low point in the middle is the anisotropy. The window length is 18m, and the log used is AT90 from the induction tool.

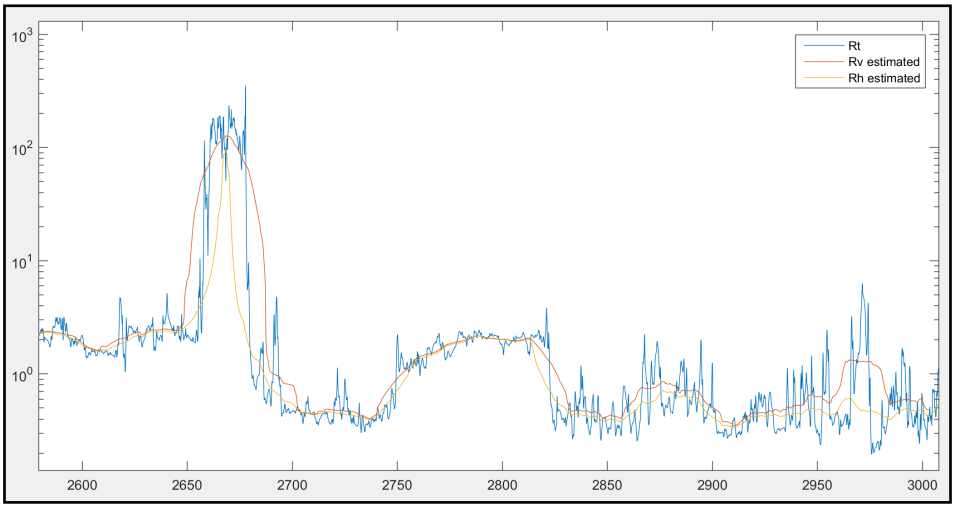

Figure 4.10: Rv and Rh estimation with an average filter of 18m over AT90 of well 3. Big scale. X axis in m and Y axis in ohm.m.

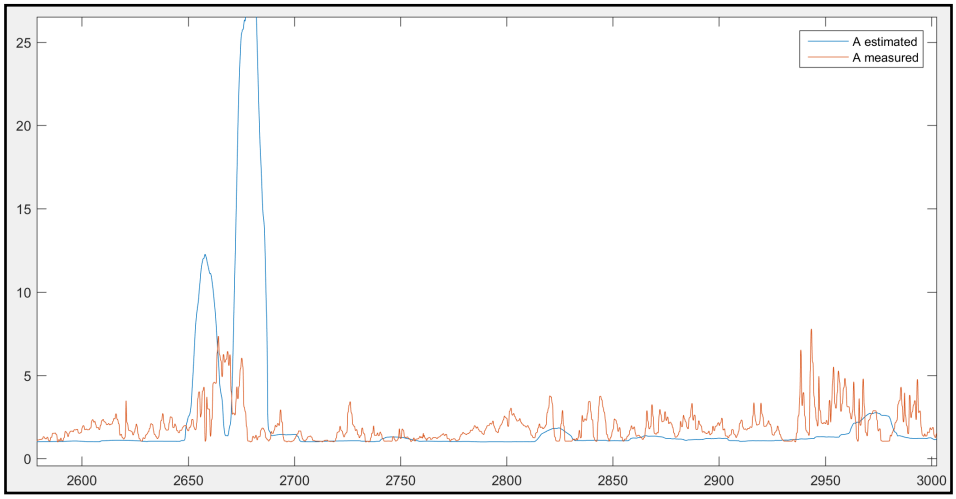

Figure 4.11: Anisotropy estimation with an average filter of 18m over AT90 of well 3. Big scale. X axis in m and Y axis is the ratio of R_v/R_h.

4.1.4 Well 4

This well is OBM and it has 40m of oil in a low anisotropic reservoir. However, a Triaxial induction tool has been used, so it is possible to compare the result of the average filter with the measured anisotropy.

Fig. 4.12 shows R_v and R_h estimation from RXOI log with a window length of 8m in the big scale, and **Fig. 4.13** shows the anisotropy estimation with the same filter. This short filter has been used thanks to the high resolution log. This window has 300 measures, which is enough for analysing the anisotropy.

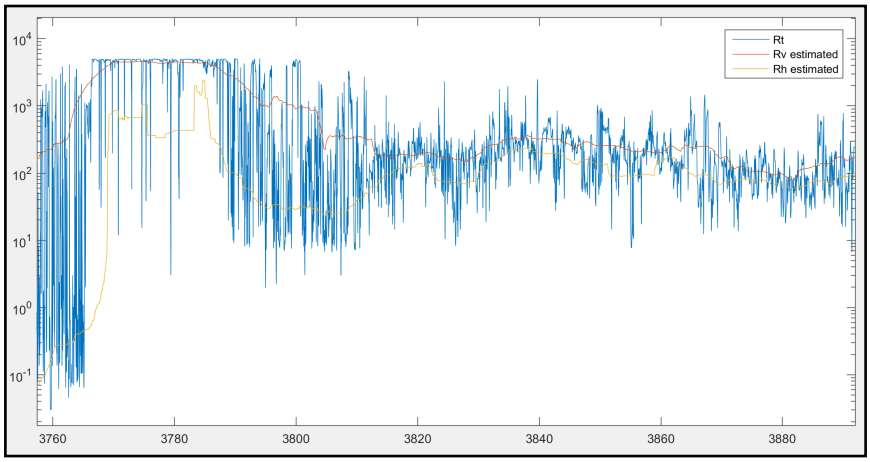

Figure 4.12: Average filter of 8m applied over RXOI in well 4. Big scale. X axis in m and Y axis in ohm.m.

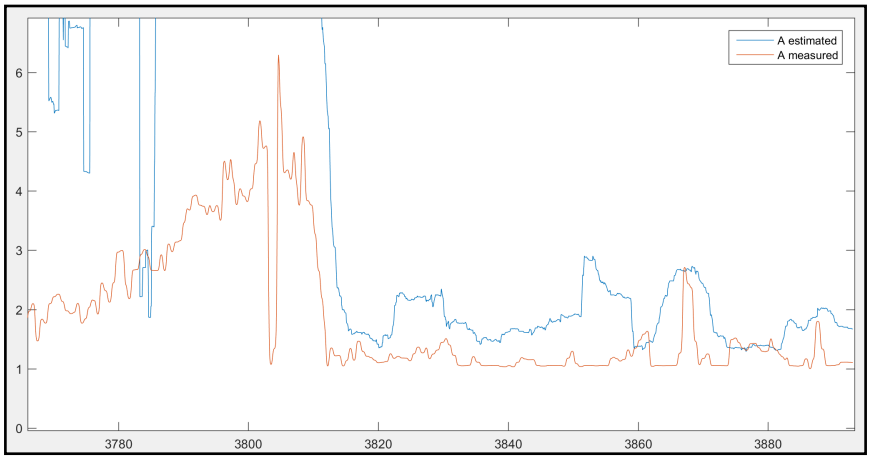

Figure 4.13: Average filter of 8m applied over RXOI in well 4. Big scale. X axis in m and Y axis is the ratio of R_v/R_h.

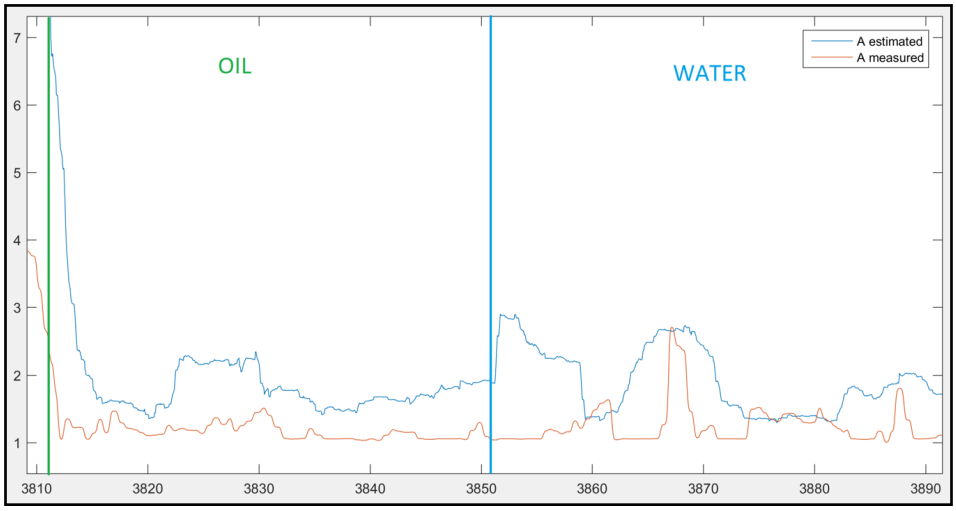

Figure 4.14: Average filter of 8m applied over RXOI in well 4 along the reservoir. X axis in m and Y axis is the ratio of R_v/R_h.

Fig. 4.14 shows the anisotropy calculation along the reservoir, where we can see that the result is an overestimation of the Triaxial induction tool result with an acceptable error, there are some zones where it has the same shape but higher values, like in 3825 and 3885. There are other zones where it reaches the measured value, like in 3367 and 3387. In these zones the important value is the peak, because 4 m in both sides are the boundary effects. It did not show the reservoir in the big scale, however, the anisotropy in the reservoir is very low, so it is hard to difference even with the Triaxial Induction Tool result.

4.1.5 Well 5

The well 5 is a WBM well that has 30m of gas and 50m of oil. The results over AT90 with a window length of 20m have been satisfactory until the last part of the reservoir, where it does not shows any anisotropy. If we remove the boundary effects, in the gas zone we can see an anisotropy of 2, in the oil zone it increases until 6 because of the thin layer of sand of 1m, and then it goes to 1 until the end of the reservoir. If we compare this results with the measured anisotropy we can see that there are some similarities. This is shown on **Fig. 4.15**. **Fig. 4.16** show how it works in the big scale, which is satisfactory, because the high value in 1430 is a noise that should be removed.

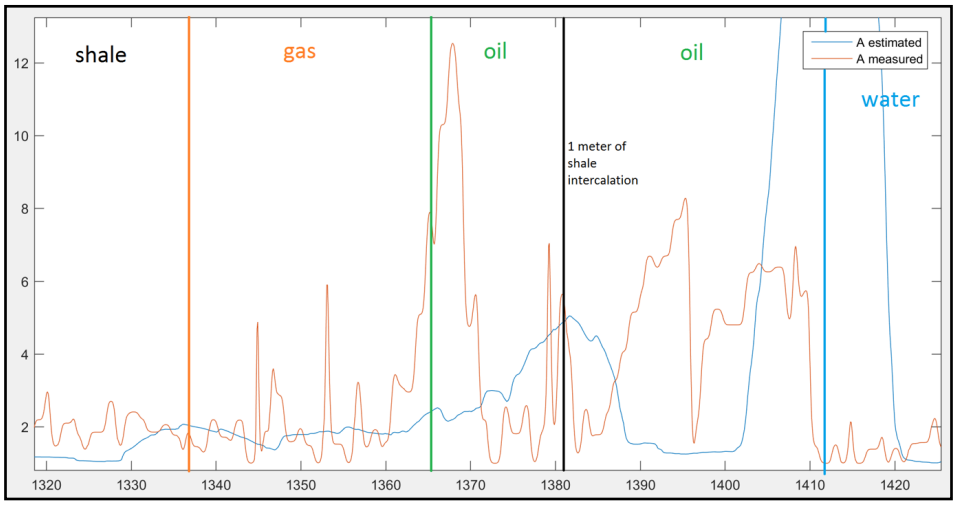

Figure 4.15: Average filter of 20m applied over AT90 log of well 5 along the reservoir. X axis in m and Y axis is the ratio of R_v/R_h.

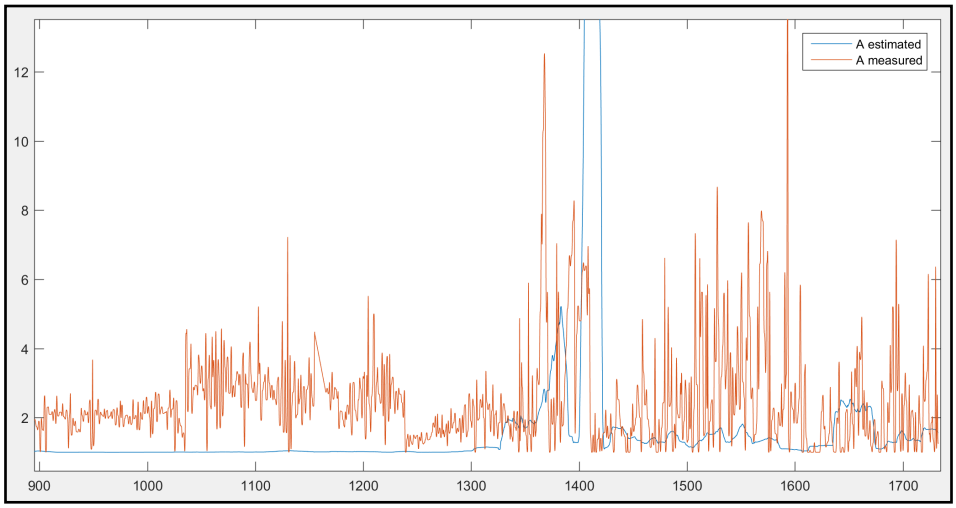

Figure 4.16: Average filter of 20m applied over AT90 log of well 5. Big scale. X axis in m and Y axis is the ratio of R_v/R_h.

4.1.6 Well 6

Well 6 is a WBM well that shows a very thick reservoir, with 50m of gas and 100m of oil. The algorithm has been tried in laterolog and induction tools with a window length of 50m. **Fig. 4.17** and **Fig. 4.18** are the results of applying it over the HRLT logs, the first one in the deep response and the second one in the shallow response. The comparison with the measured anisotropy is not bad, but there are some zones where the anisotropy is expected to be high, but it is just one.

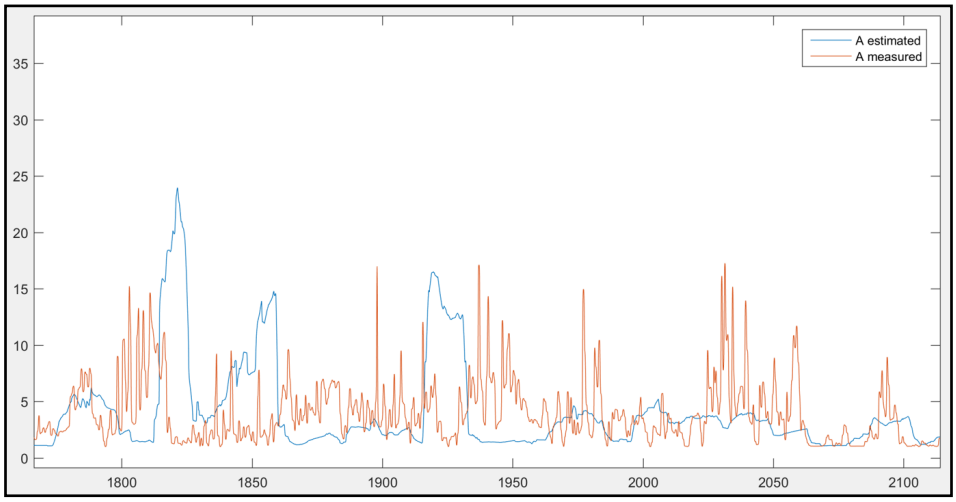

Figure 4.17: Average filter of 50m applied over deep resistivity from HRLT, in well 6 along the reservoir. X axis in m and Y axis is the ratio of R_v/R_h.

Fig. 4.19 shows the response over AT90 log, we can see that the response is more uniform that the HRLT tool and there is not any point that has an anisotropy of 1 along the reservoir.

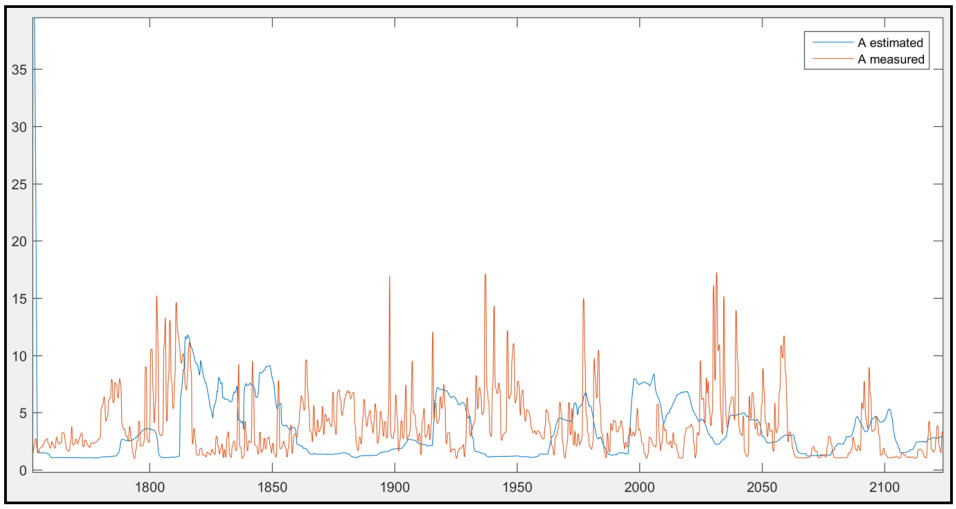

Figure 4.18: Average filter of 50m applied over shallow resistivity from HRLT, in well 6 along the reservoir. X axis in m and Y axis is the ratio of R_v/R_h.

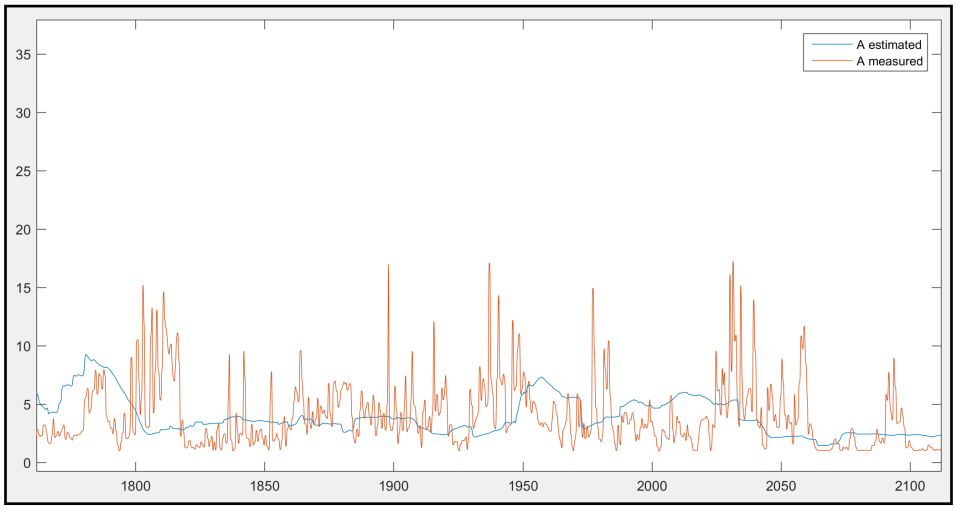

Figure 4.19: Average filter of 50m applied over AT90, from well 6 along the reservoir. X axis in m and Y axis is the ratio of R_v/R_h.

4.2 Method 2: estimating Rv from the estimation of the resistivity of the sand.

4.2.1 Well 1

This method, explained in chapter 3, has been applied over well 1, with a resistivity of the shale of 4 ohm.m (from the top of the reservoir) and a window length of 1.5m. **Fig. 4.20** shows the anisotropy calculated from RXOI. The problem is that this well is WBM, so most of the oil has been pushed by the mud and the resistivity values close to the well are very low, as a consequence, the anisotropy is very low too. Because of this, in a WBM well a deep resistivity log must be used.

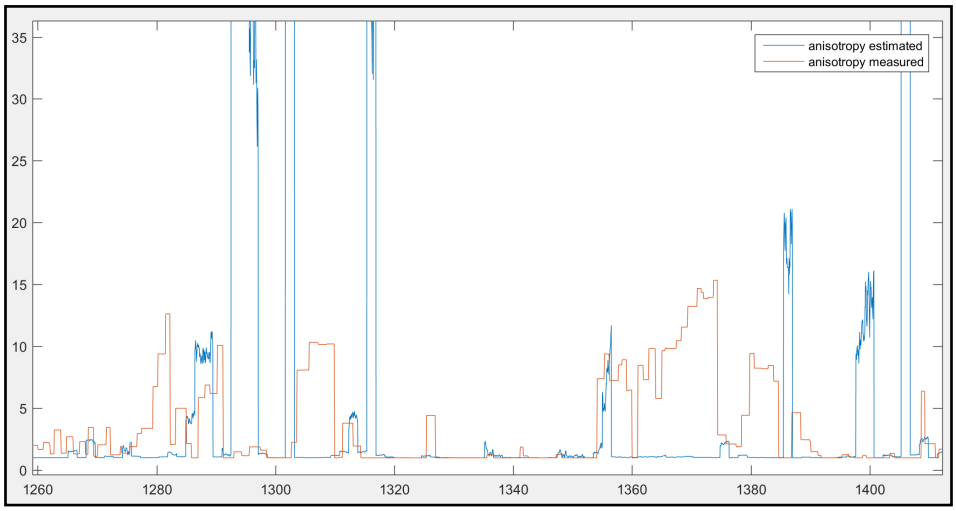

Figure 4.20: Anisotropy estimated in the reservoir of well 1 from RXOI, estimating R_s. X axis in m and Y axis is the ratio of R_v/R_h.

The same algorithm has been applied over the deep resistivity measured by HRLT tool, with a resistivity of the shale of 4 ohm.m and a window length of 1.5m.

The result, shown on **Fig. 4.21**, shows that the correlation is not very satisfactory. **Fig. 4.22** and **Fig. 4.23** show the result over AT90, which is similar to the HRLT result.

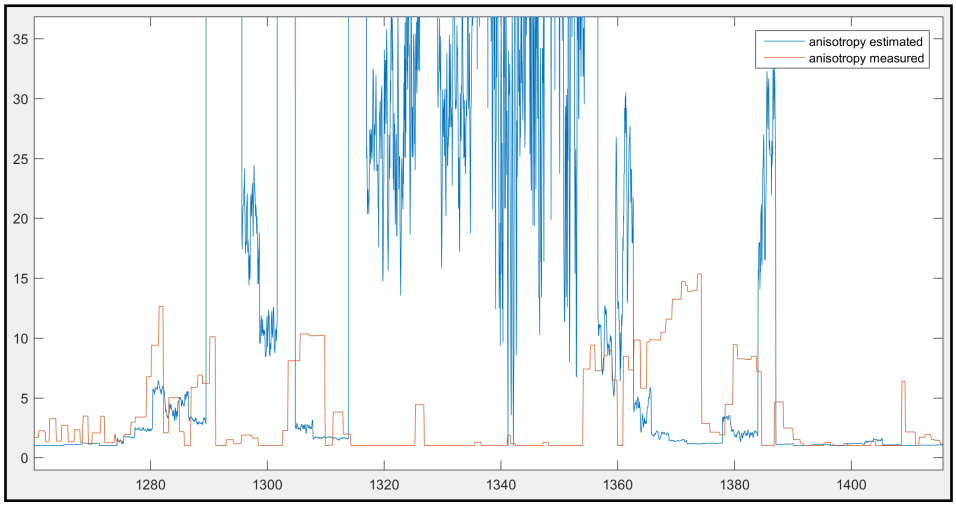

Figure 4.21: Anisotropy estimated in the reservoir of well 1 from HRLT, estimating R_s. X axis in m and Y axis is the ratio of R_v/R_h.

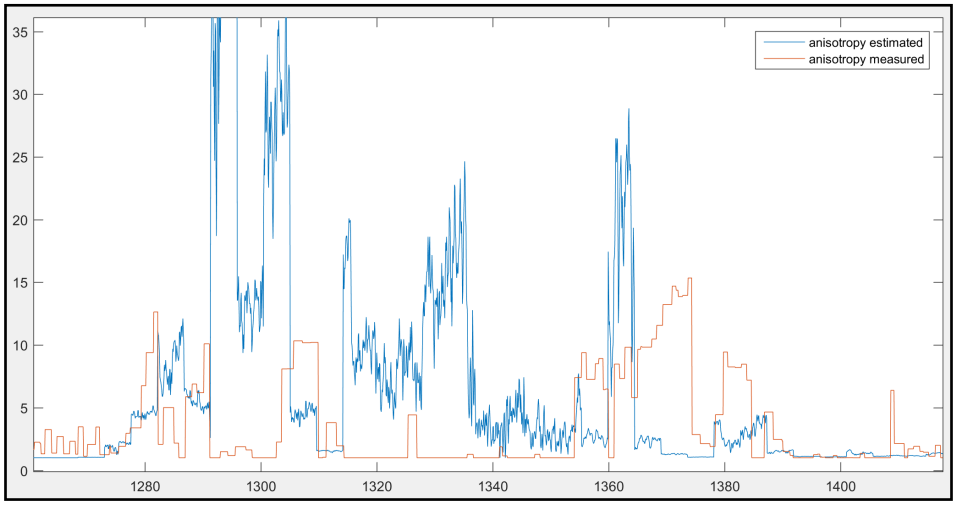

Figure 4.22: Anisotropy estimated in the reservoir of well 1 from AT90, estimating R_s. X axis in m and Y axis is the ratio of R_v/R_h.

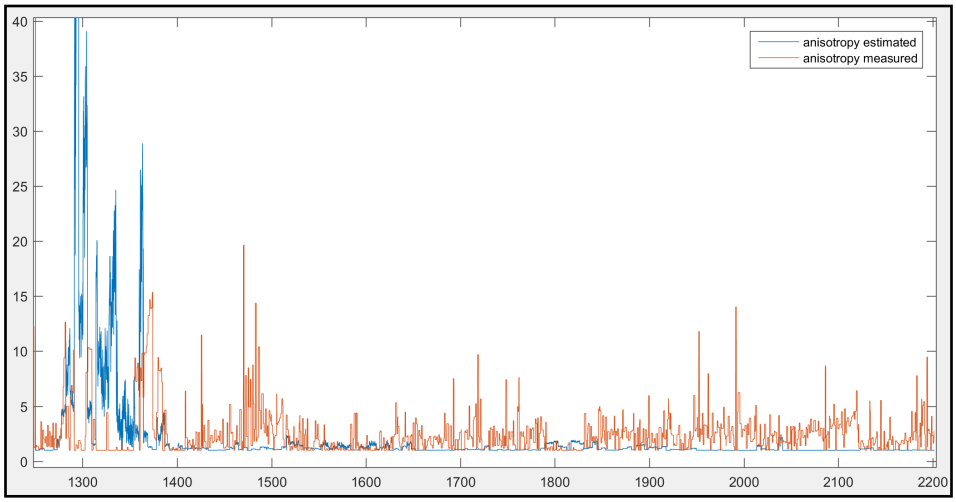

Figure 4.23: Anisotropy estimated in the well 1 from AT90 in the big scale, estimating R_s. X axis in m and Y axis is the ratio of R_v/R_h.

4.2.2 Well 2

As it has been mentioned before, this well does not have the anisotropy measured by Triaxial Induction Tool, however, the method has been tried here too. The results looks satisfactory applying a small window length of 3m, getting an anisotropy between 4 and 8 along the reservoir, as it is shown on **Fig. 4.24**.

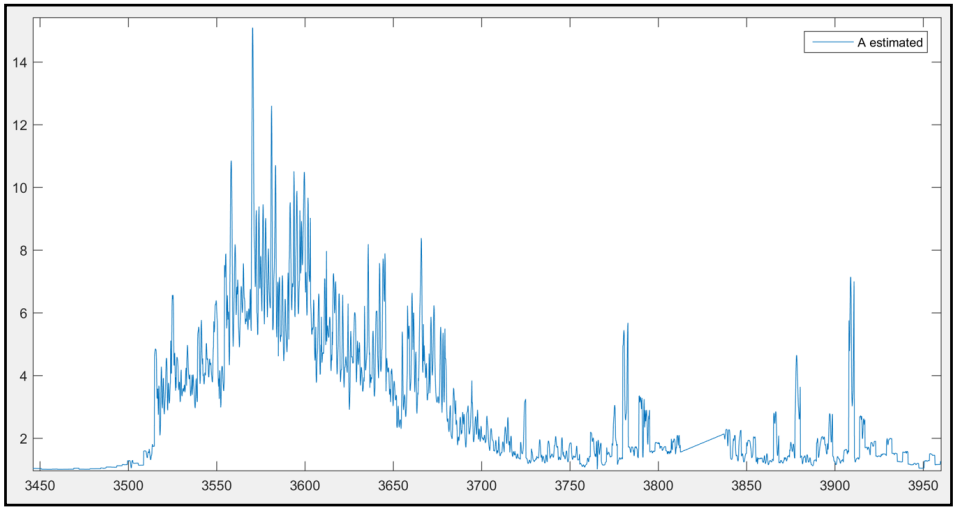

Figure 4.24: Anisotropy estimated in well 2 from shallow resistivity along the reservoir, estimating R_s. X axis in m and Y axis is the ratio of R_v/R_h.

This has been applied in the shallow resistivity because it is the one with higher resolution, nevertheless, this tool has been applied only along the reservoir, and for measuring the big scale the algorithm has to be applied over the deep resistivity, as it is shown on **Fig. 4.25**. On **Fig. 4.26** shows that the difference with the shallow resisitivity is not important, both show similar values of anisotropy.

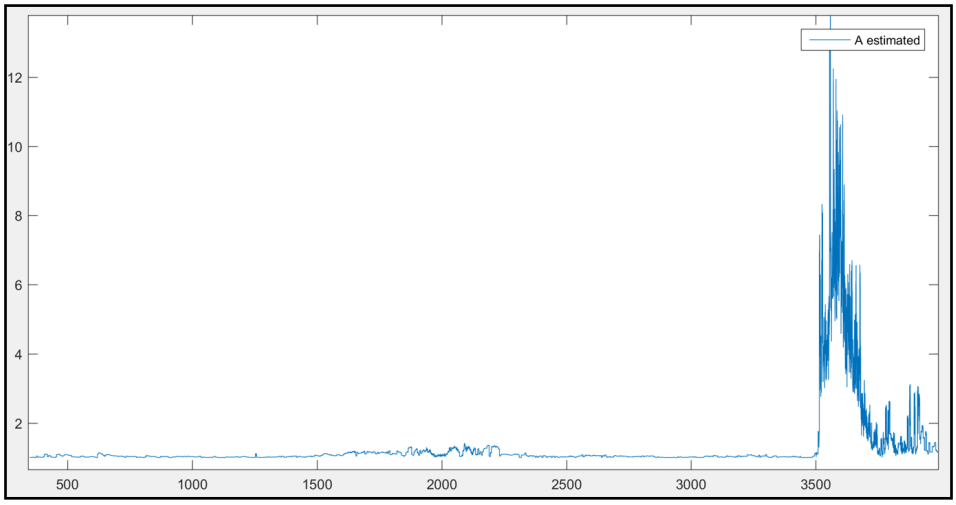

Figure 4.25: Anisotropy estimated in well 2 from deep resistivity in the big scale, estimating R_s. X axis in m and Y axis is the ratio of R_v/R_h.

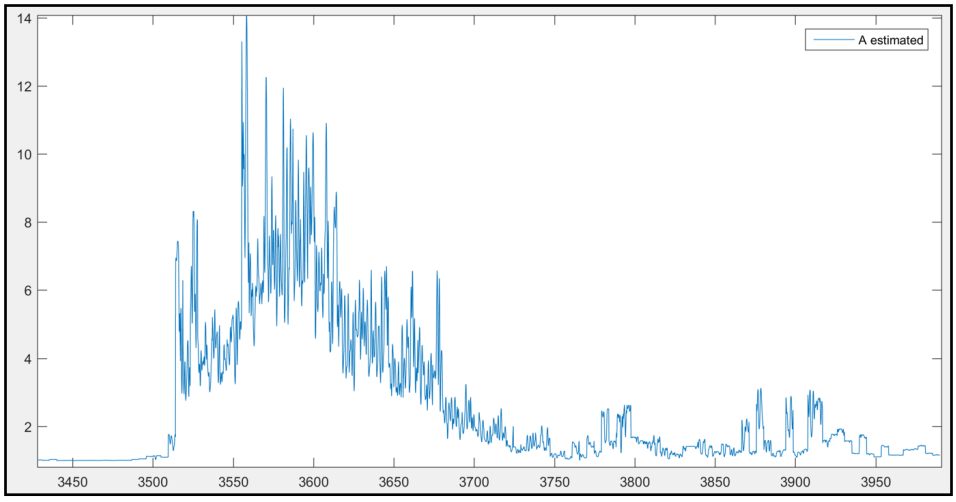

Figure 4.26: Anisotropy estimated in well 2 from deep resistivity along the reservoir, estimating R_s. X axis in m and Y axis is the ratio of R_v/R_h.

4.2.3 Well 3

The method has been applied over well 3 with a resistivity of the shale of 2 ohm.m (from the shale on top of the reservoir). **Fig. 4.27** shows the anisotropy calculation, which is not perfectly the same as the one calculated from the Triaxial tool, but it shows something similar.

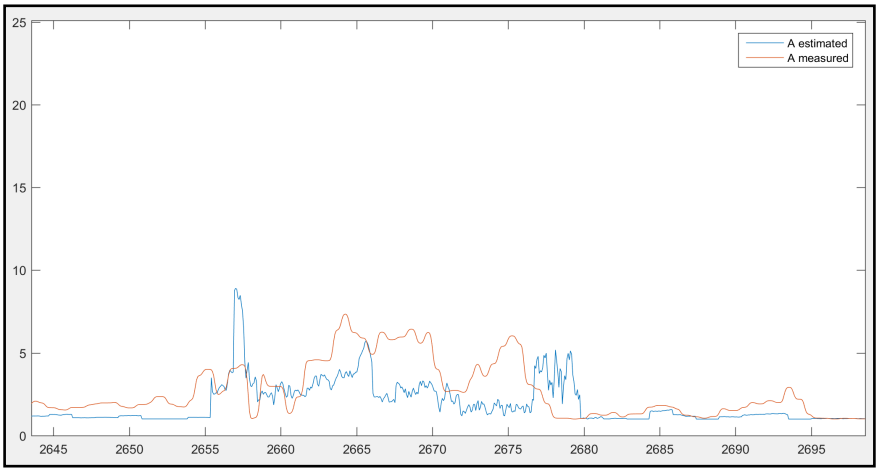

Figure 4.27: Anisotropy estimated in the reservoir of well 3 from AORX, estimating R_s. X axis in m and Y axis is the ratio of R_v/R_h.

If we analyse the signal on the big scale, we can see that the shale anisotropy does not affect this method and the anisotropic reservoir has been identified very well. This is shown on **Fig. 4.28**

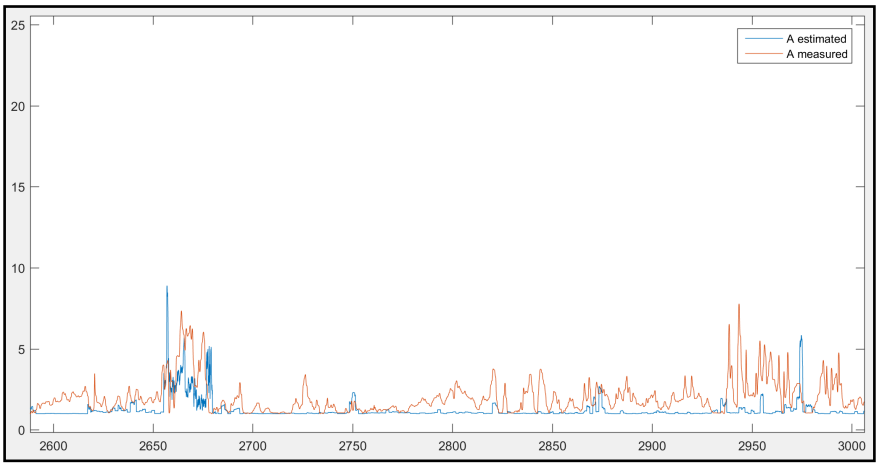

Figure 4.28: Anisotropy estimated in well 3 from AORX in the big scale, estimating R_s. X axis in m and Y axis is the ratio of R_v/R_h..

4.2.4 Well 4

The algorithm applied along the AT10 log from well 4, with a resistivity of the shale of 2 ohm.m (the top of the reservoir), shows a satisfactory result, the anisotropy shown is very similar to the measured one, even the peaks in 3850m and 3867m are shown with this algorithm too. **Fig. 4.29**.

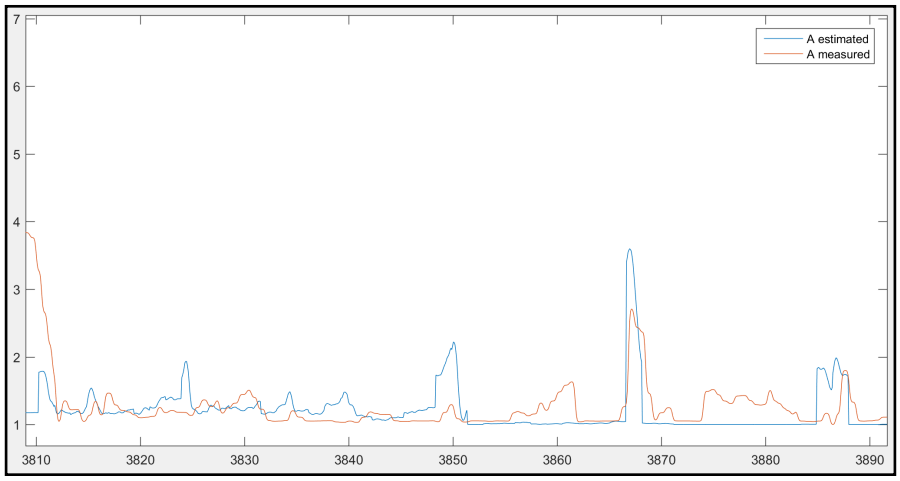

Figure 4.29: Anisotropy estimated in the reservoir of well 4 from AT10, estimating R_s. X axis in m and Y axis is the ratio of R_v/R_h.

Fig. 4.30 shows how it works on the big scale. It is not affected by the anisotropy of the shale and the result is quite uniform.

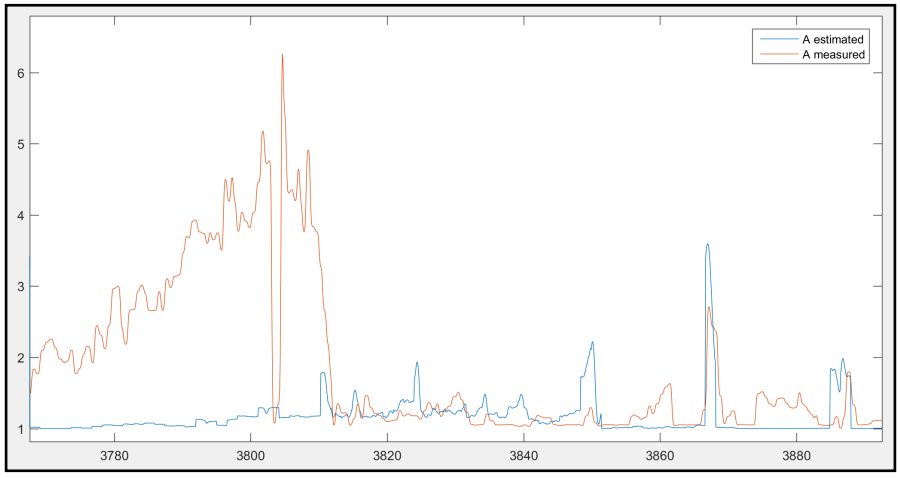

Figure 4.30: Anisotropy estimated in well 4 from AT10 in the big scale, estimating R_s. X axis in m and Y axis is the ratio of R_v/R_h.

4.2.5 Well 5

On **Fig. 4.31** we can see the result over AT90, with a resistivity of the shale of 2 ohm.m (the top of the reservoir), there are parts where it fits better, like in the beginning of the reservoir, from 1340m to 1365m, and from 1380m to 1395m. **Fig. 4.32** shows how the anisotropic zone is recognized in the big scale.

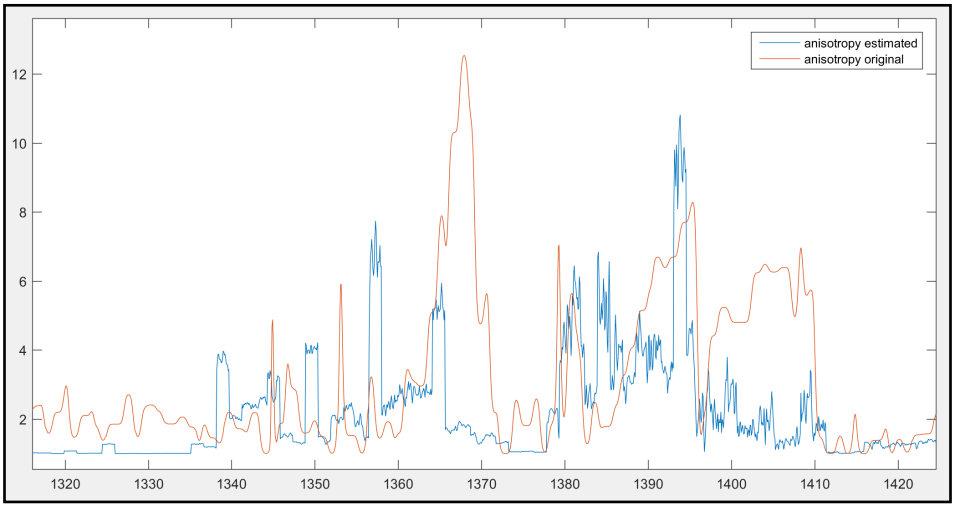

Figure 4.31: Anisotropy estimated in the reservoir of well 5 from AT90, estimating R_s. X axis in m and Y axis is the ratio of R_v/R_h.

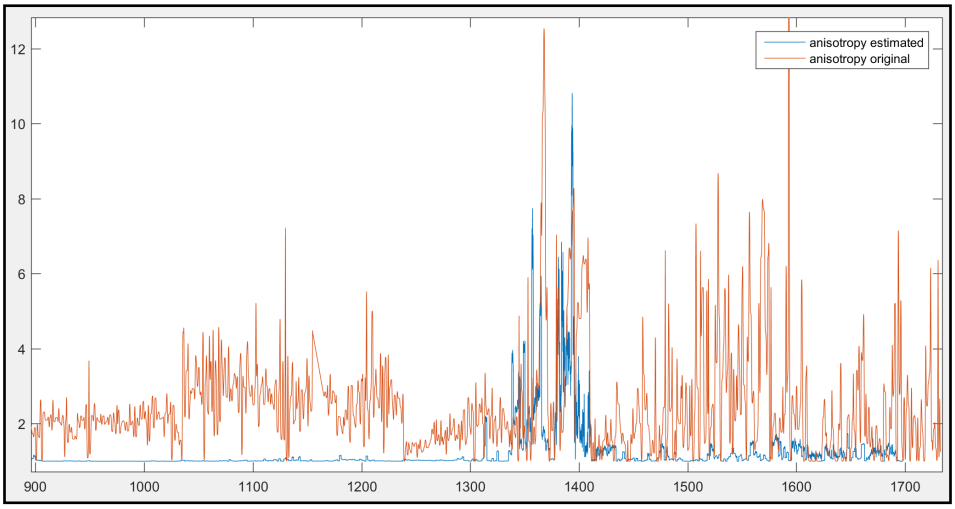

Figure 4.32: Anisotropy estimated in well 5, from AT90, in the big scale, estimating R_s. X axis in m and Y axis is the ratio of R_v/R_h.

4.2.6 Well 6

The algorithm shows an unexpected result along this well, a resistivity of 10 ohm.m for the shale is needed to be set for getting reasonable values. The AT90 (**Fig. 4.33**) shows peaks that reach more or less the values that the measured anisotropy, however, if we use the deep resistivity from HRLT, we only get the zone where there is anisotropy, but the values are much higher than the measured anisotropy (**Fig. 4.34**).

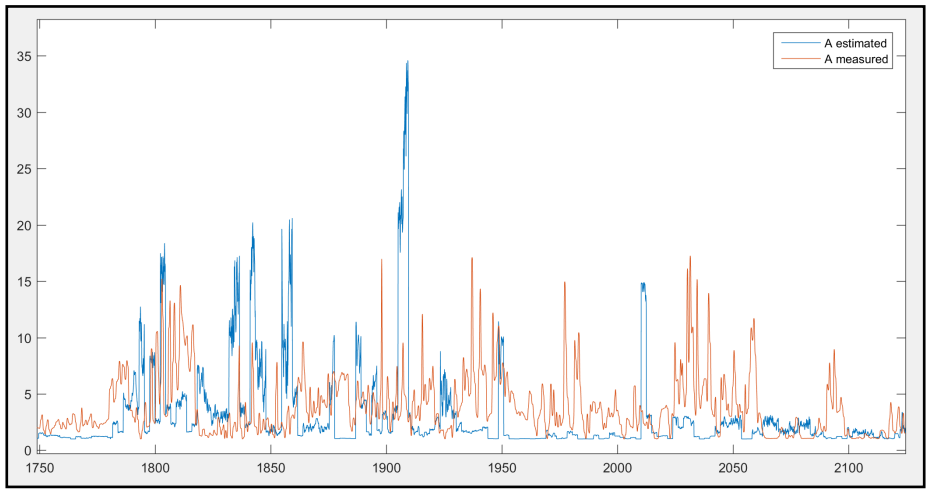

Figure 4.33: Anisotropy estimated in the reservoir of well 6 from AT90, estimating R_s. X axis in m and Y axis is the ratio of R_v/R_h.

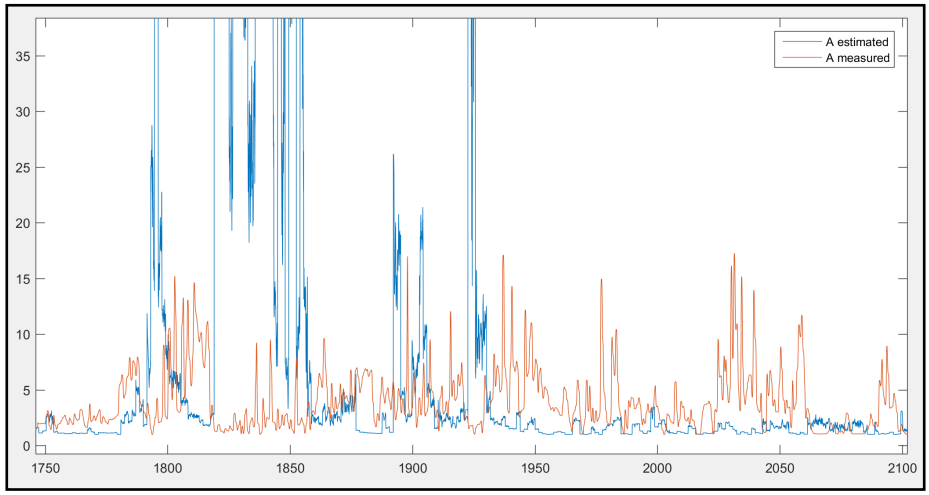

Figure 4.34: Anisotropy estimated in the reservoir of well 6 from HRLT, estimating R_s. X axis in m and Y axis is the ratio of R_v/R_h.

4.3 Method 3: estimating Rv from deep resistivity and GR tool.

4.3.1 Well 1

Using the method explained in chapter 3, a window length of 2.5m, and different shale resistivities, ranging from 3 to 5.5 ohm.m that are read in the thicker shale, we obtain the results shown on **Fig. 4.35**, where we can compare it with the vertical resistivity measured by the Triaxial Induction tool.

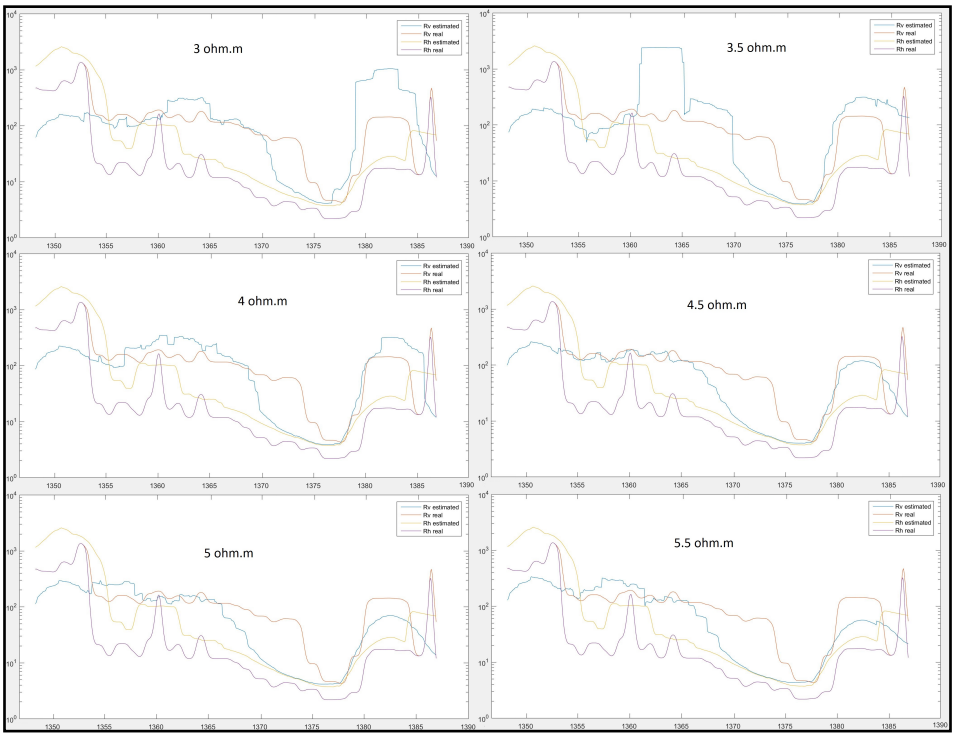

Figure 4.35: Comparison of Rv and Rh estimated in the interesting zone of well 1, using GR and HRLT. X axis in m and Y axis in ohm.m.

Fig. 4.36 shows the anisotropy measured by the Triaxial Induction tool with the anisotropy estimated by this method with a resistivity of the shale of 4 ohm.m.

This method is going to be analyzed now in the big scale, this can be seen on **Fig. 4.37**, where the thin laminated reservoir has been identified at 1370m.

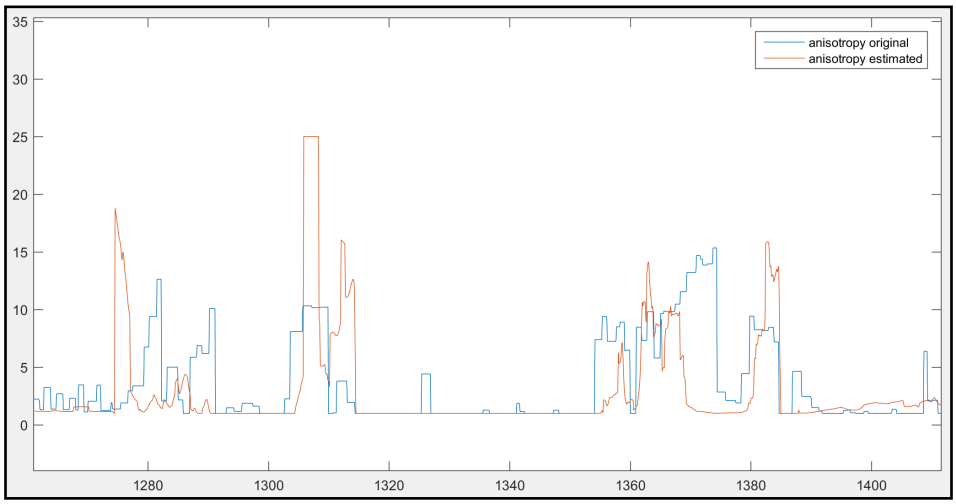

Figure 4.36: Anisotropy estimated in the interesting zone of well 1, using GR and HRLT. X axis in m and Y axis is the ratio of R_v/R_h.

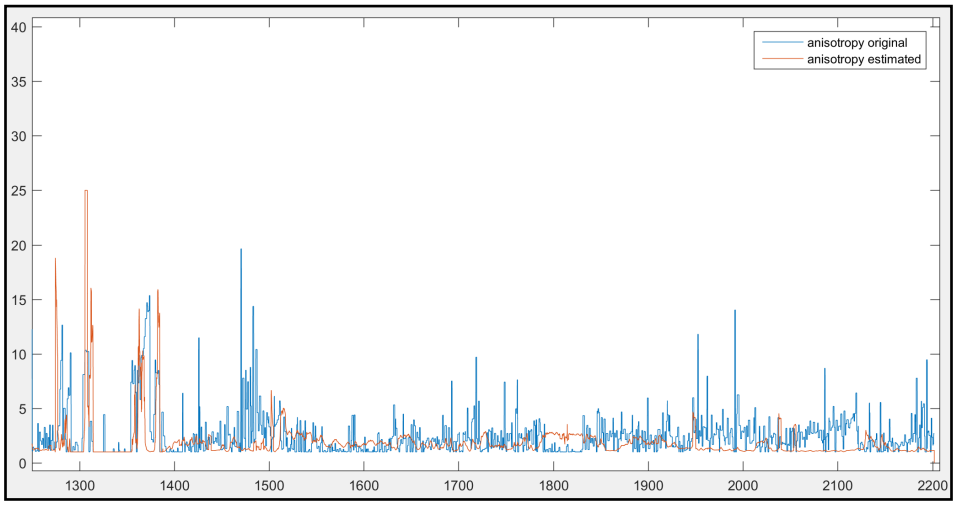

Figure 4.37: Anisotropy estimated in the big scale in well 1, using GR and HRLT. X axis in m and Y axis is the ratio of R_v/R_h.

The method has been tried in AT90, with satisfactory results too. **Fig. 4.38** shows the result along the reservoir, where an average filter of 10m has been used because the original curve was very spiky. **Fig. 4.39** shows the result in the big scale, which is satisfactory too.

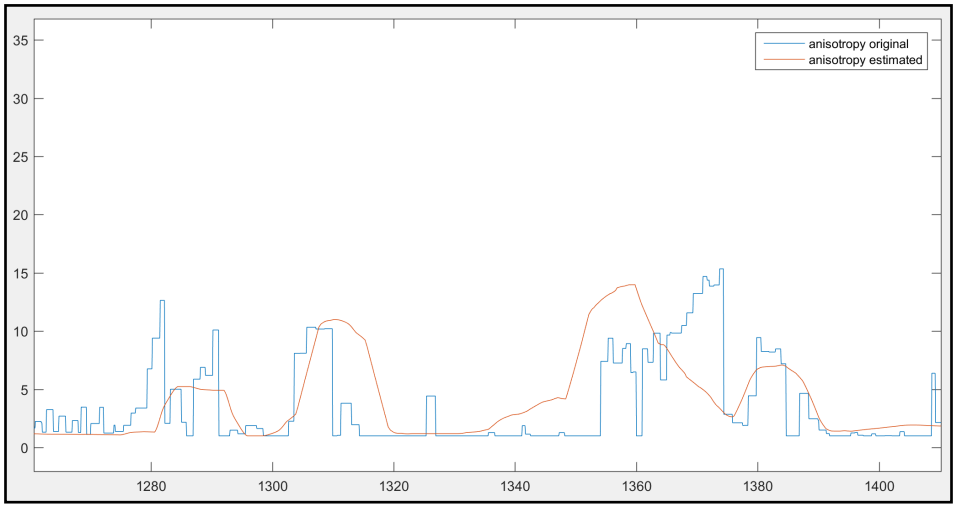

Figure 4.38: Anisotropy estimated in the interesting zone of well 1, using GR and AT90. X axis in m and Y axis is the ratio of R_v/R_h.

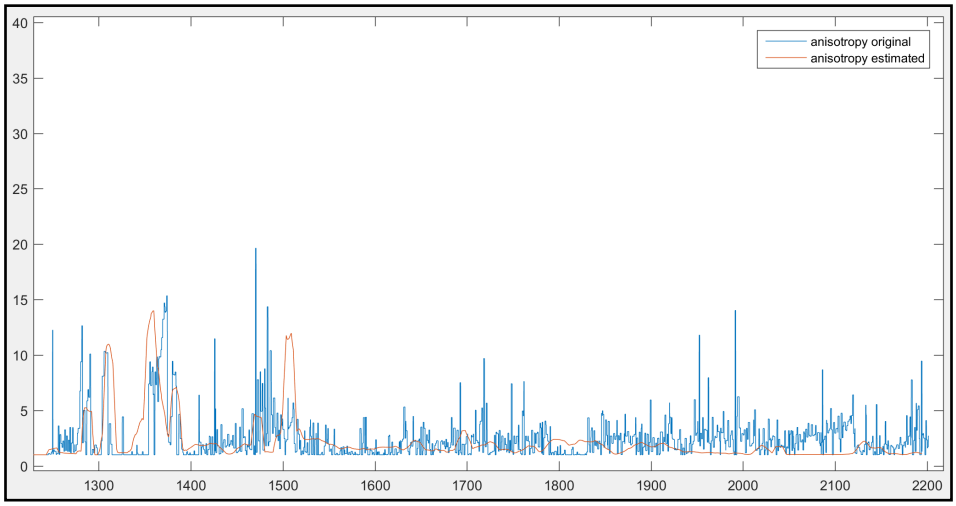

Figure 4.39: Anisotropy estimated in the big scale in well 1, using GR and AT90. X axis in m and Y axis is the ratio of R_v/R_h.

4.3.2 Well 2

The algorithm has been applied over well 2, the one that does not have a Triaxial Induction tool for comparison. The result along the reservoir can be seen on **Fig. 4.40**. **Fig. 4.41** shows how it works in the big scale. The algorithm identifies the reservoir very well, but the values of anisotropy are very high.

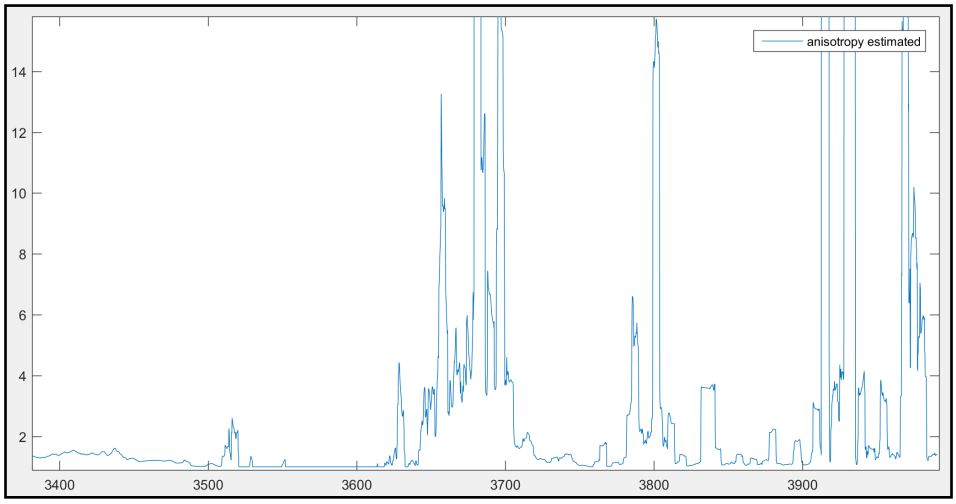

Figure 4.40: Anisotropy along the reservoir of well 2, using GR and deep resistivity. X axis in m and Y axis is the ratio of R_v/R_h.

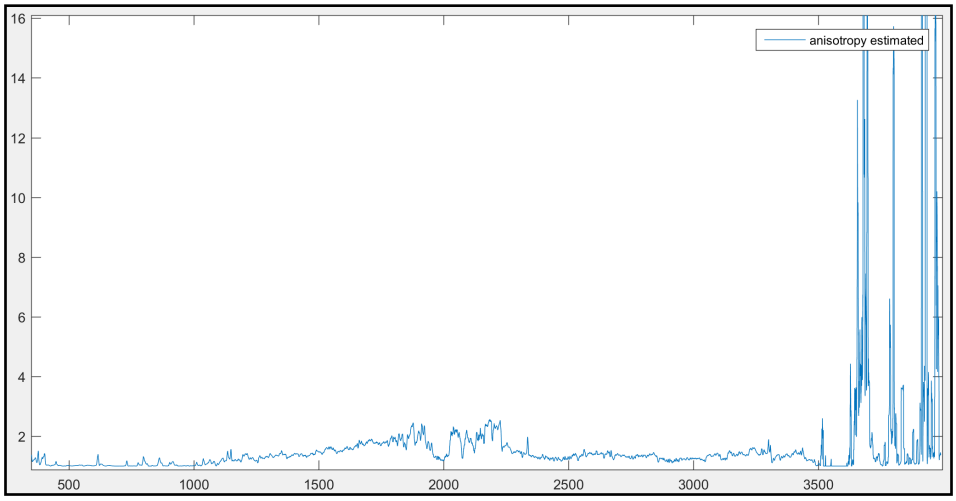

Figure 4.41: Anisotropy estimated in the big scale in well 2, using GR and deep resistivity. X axis in m and Y axis is the ratio of R_v/R_h.

4.3.3 Well 3

The same method has been applied over AT90 of well 3 with a resistivity of the shale of 2 ohm.m (the top of the reservoir) and a window length of 2.2 m. On **Fig. 4.42** we can see that the estimation of Rv is quite satisfactory in both extremes of the reservoir, the reason for having that low Rv in the middle of the reservoir is because of the increment in the volume of shale. It looks like it does not affect Rv calculation from the Triaxial induction tool. **Fig. 4.42** shows the anisotropy estimation along the reservoir

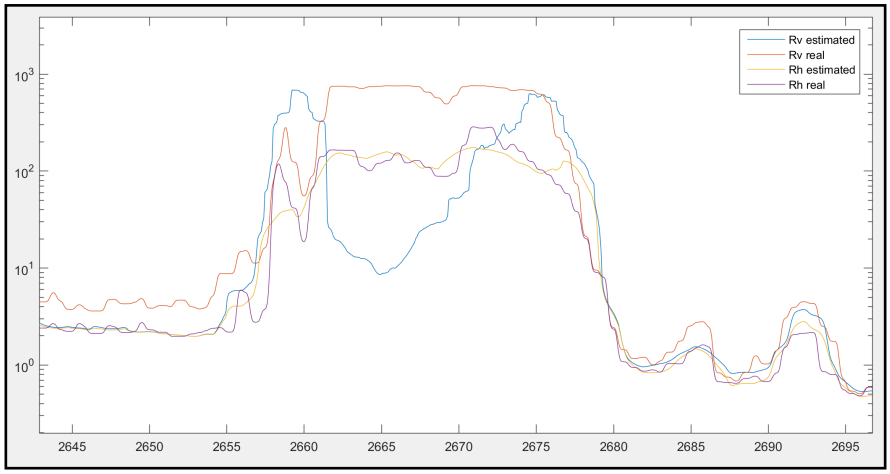

Figure 4.42: Estimation of Rv in well 3, along the reservoir, using GR and AT90. X axis in m and Y axis in ohm.m.

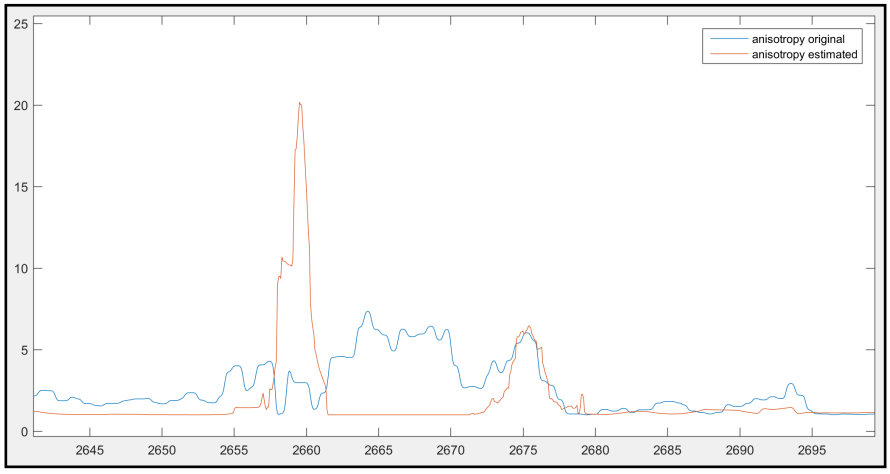

Figure 4.43: Anisotropy estimated along the reservoir of well 3, using GR and AT90. X axis in m and Y axis is the ratio of R_v/R_h.

On **Fig. 4.44** we can see that the anisotropy estimated is not affected by the anisotropy of the shale. The estimation of the anisotropy along the reservoir, as it is said before, it fits really well the measured value in the bottom of the reservoir.

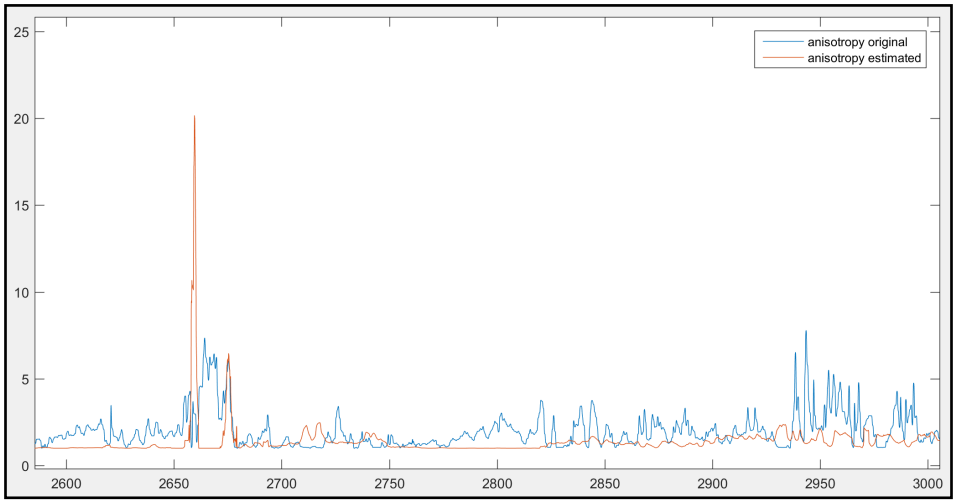

Figure 4.44: Anisotropy estimated in the big scale in well 3, using GR and AT90. X axis in m and Y axis is the ratio of R_v/R_h.

4.3.4 Well 4

Applying the algorithm over AT90 of this low anisotropy reservoir, we can see that more or less it follows the shape of the measured anisotropy curve along the oil zone (OWC at 3860m). **Fig. 4.45** shows the results of this experiment. This has been calculated with a resistivity of the shale of 2 ohm.m (read in the top of the reservoir). **Fig. 4.46** shows the result in the big scale.

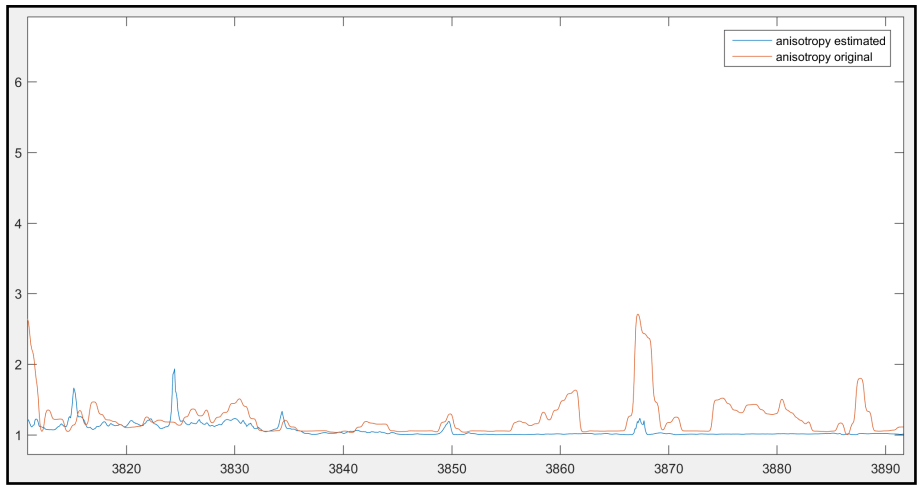

Figure 4.45: Anisotropy estimated in the reservoir of well 4, using GR and AT90. X axis in m and Y axis is the ratio of R_v/R_h.

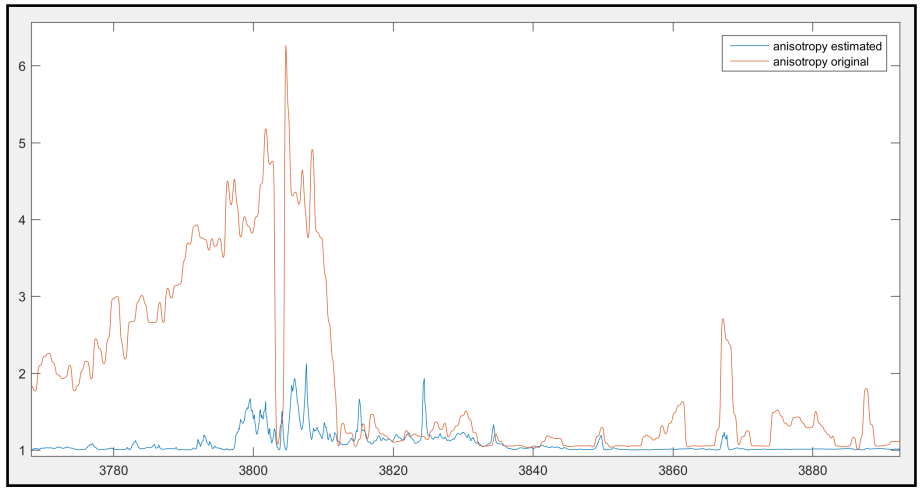

Figure 4.46: Anisotropy estimated in well 4 in the big scale, using GR and AT90. X axis in m and Y axis is the ratio of R_v/R_h.

4.3.5 Well 5

The algorithm shows a satisfactory result along the reservoir of well 5, having high values and low values where it is expected. **Fig. 4.47** shows this result from AT90 with a length of the window of 5m and a resistivity of the shale of 2 ohm.m (read in the top of the reservoir). **Fig. 4.48** shows the result in the big scale, where the thick shales do not have any effect on the anisotropy. The two peaks at 1280m and 1440m are due to noise in the GR log.

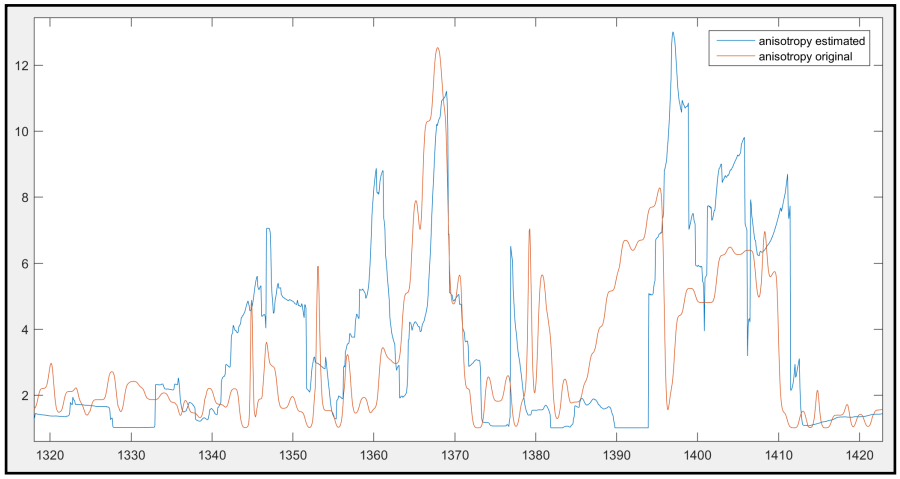

Figure 4.47: Anisotropy estimated in the reservoir of well 5, using GR and AT90. X axis in m and Y axis is the ratio of R_v/R_h.

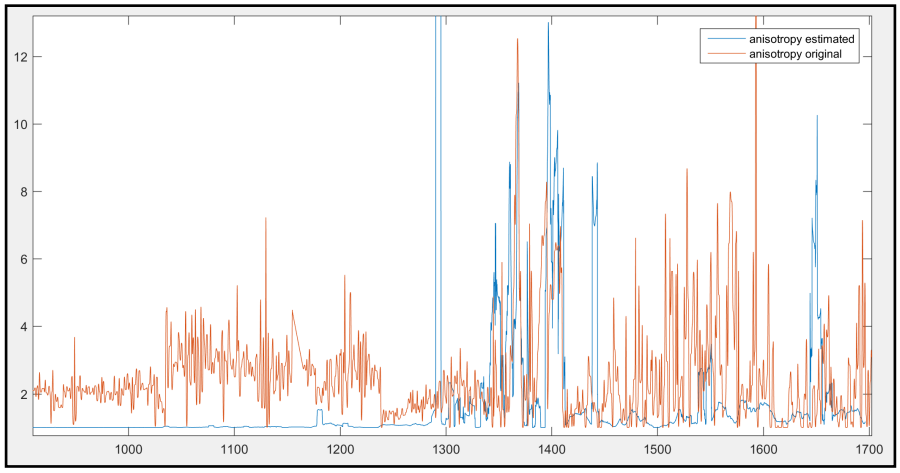

Figure 4.48: Anisotropy estimated in well 5 in the big scale, using GR and AT90. X axis in m and Y axis is the ratio of R_v/R_h.

4.3.6 Well 6

The algorithm has been applied over the deep resistivity log from HRLT (**Fig. 4.49**) and over AT90 (**Fig. 4.50**) with a length window of 2.5m, both results are not very satisfactory and a resistivity of 10 ohm.m has been used for the shale for getting reasonable values, but it is not real. The first one has anisotropies with very high peaks and some intervals do not show any anisotropy when it expected to be high, however, some zones fits well with the measured anisotropy. The response to the AIT tool is similar, there are some high values that are very far from the measured anisotropy and others where it does not shows any anisotropy where it is expected, but there are some areas where the error is not big, like from 1800m to 1860 and from 1920m to 1940m.

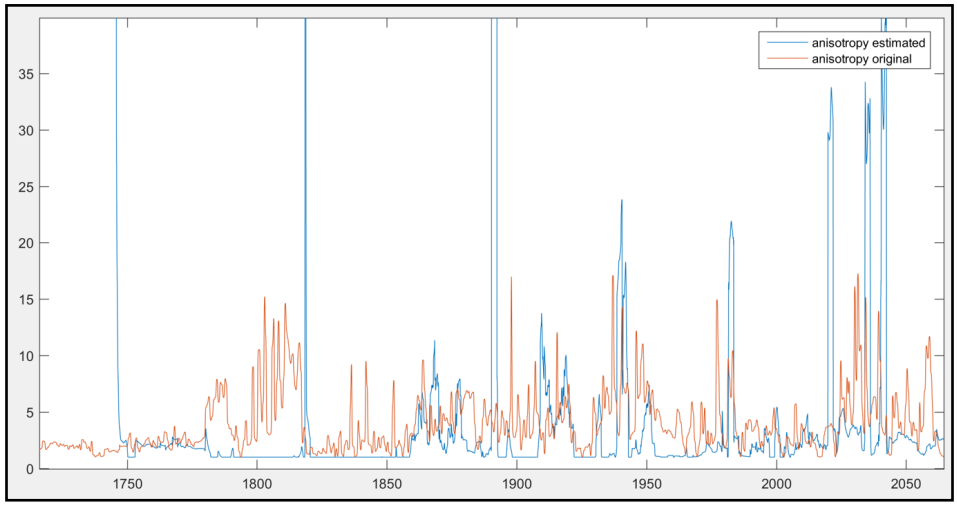

Figure 4.49: Anisotropy estimated in the reservoir of well 6, using GR and HRLT. X axis in m and Y axis is the ratio of R_v/R_h.

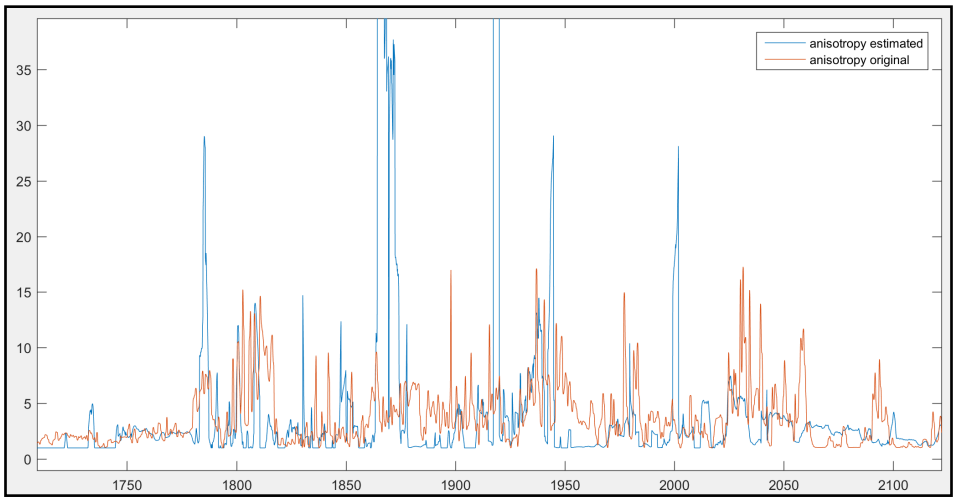

Figure 4.50: Anisotropy estimated in the reservoir of well 6, using GR and AT90. X axis in m and Y axis is the ratio of R_v/R_h.

Chapter 5

Discussion

5.1 Method 1: estimating Rv from a convolution average filter.

On well 1 the method works quite well using the AT90 signal. It looks like the result is an average of the anisotropy measured by the Triaxial Induction Tool, giving an anisotropy of 4 along all the well.

On well 2 is not possible to compare the anisotropy because the Triaxial Induction Tool was not used, however, it has been a good example for proving how the algorithm reacts to changes in lithology, which is what was expected from the theory explanation in chapter 3.

Well 3 was not really useful because the reservoir was only 10m of oil and 10m of gas, so a very small window was needed for having more results than boundary effects. However, this well shows the limitation of the method.

Well 4 was the only OBM well with RXOI log available. This is because very high resolution measurements are normally taken by the MicroSFL (MSFL) device, that is a pad-mounted spherically focused logging sensor that measures sending an electrical current to the formation. Normally, in an OBM well the mudcake formed is so thick that the resistivity is very high and the current sent by MSFL can not reach the formation, so the log resulting from this measurement is very unrealistic. Companies usually remove the log from the data base due to the uselessness of it, and this is the reason why OBM wells usually do not have a very high resolution resistivity measurement. This does not occur in a WBM well because the mudcake formed in the wall of the well is still conductive. Nevertheless, if the cake is very thin in an OBM well, like well 4, it will have available a RXOI log. In this well, the best result has been obtained by this method. Although the measured anisotropy of the reservoir is very low, the anisotropy estimated by the algorithm is very satisfactory, following the same shape of the curve with a small error.

Wells 5 and 6 have similar results as well 1. They have in common that they are WBM and the algorithm has been applied over AT90. The result appears as an average of the

measured anisotropy along the reservoir, showing anisotropies between 2 and 6.

Analyzing this method in the big scale, the reservoir can be clearly identified because it is the only part where the anisotropy is high. The values outside the reservoir are always between 1 and 2. If the values are higher than that, it can occur because of noise or bad data acquisition. The isotropic reservoir of well 4 was not identified as an anisotropic reservoir, so this is a good result.

5.2 Method 2: estimating Rv from the estimation of the resistivity of the sand.

This method did not work well in the well 1, the estimated anisotropy is very low where is expected to be high, and there are peaks that reach values of 30 and 40 values. In this well, the only positive result was the identification of the reservoir.

On well 2 is not possible to compare the anisotropy, however, the result reach expected values, an anisotropy between 4 and 8 along the reservoir, and an anisotropy of 2 in the water saturated part of the reservoir. In all shale the anisotropy is 1.

Results were satisfactory in well 3 too, where the anisotropy is 1 outside the reservoir and reaching values from 3 to 6 in the anisotropic reservoir, there is a bit of error in the comparison with the Triaxial Induction tool, but it is an acceptable error.

The method worked well in well 4 too, with a very small error and showing the low anisotropy that the Triaxial Induction tool detected. Wells 2, 3 and 4, where the algorithm worked well, have in common that the mud is oil based, so this is an important fact to take into account for using this method.

The method did not work as well in the WBM wells than in the OBM wells. However, we get some spiky curves that follow the shape of the anisotropy measured by Triaxial Induction Tool in some zones, as it is shown in wells 5 and 6. Well 5 has less error than well 6, where the result is very spiky and it is hard to see the relation between the anisotropy measured and the anisotropy estimated.

As method 1, this method has worked well for identifying anisotropic reservoirs. The algorithm has distinguished the reservoir in most wells. The only well where the reservoir has not been identified is in well 4, where anisotropy does not exist and the reservoir has not been disguised, so this is a result consistent with the method.

5.3 Method 3: estimating Rv from the deep resistivity and GR tool.

The wells 1, 4 and 5 got a very satisfactory result, where the shape and the values of the estimated curves are very similar to the values calculated by the Triaxial Induction Tool, the error is small. These are the wells where the algorithm works better, and they are a mix of WBM and OBM, and HRLT and AT90, so the good result is not related to the type of mud or if it is an induction or laterolog tool.

Well 3 had a good response too, in terms of values achieved, however, the middle part of the reservoir has a lower vertical resistivity than the one computed by Triaxial Induction

Tool, this happens because of the increment in GR in that area, so maybe the anisotropy read by Triaxial Induction Tool contains the anisotropy of the shale too, or the high GR is due to other minerals and it does not mean an increase in shale.

Wells 2 and 6 are the ones where the method did not really work. The first one is only useful to identify the anisotropic reservoir, but the values are very high and very spiky. However, in the second one, some places show anisotropy that are very similar to the measured one, but other places where it is expected to be high is only 1, and there are some peaks where the anisotropy is huge, that can occur due to noise.

Like methods 1 and 2, this method has showed all the reservoirs in the big scale as they were expected. Only the reservoir of well 4 has not been distinguished, again due to the isotropic nature of the reservoir, so, this is the result that it was expected.

5.4 Comparison of all the methods

Method 1 is very useful in OBM wells with high resolution resistivity logs available, like RXOI, where the window length is not very big (around 10m). It works well because the sand layers of the reservoir get saturated with the oil mud in the wall of the well and this creates a big contrast with the low resistivity of the layers of shale, these layers are impermeable and they do not get saturated with the oil based mud. The high resolution tools read the resistivity in the wall of the well, if the mud is water based, the sand layers will be saturated in water and there will not be a enough big contrast with the resistivity of the shale. If this method is going to be applied in a WBM, the reservoir needs to be thicker than 20m and it has to be applied with a deep-reading resistivity log, showing the best results with AT90 from induction tool. The result will be an average of the anisotropy along the well. The article from Tabanou et al. (2002), where the study was only done in an OBM well with OBMI tool, shows results that are consistent with the results achieved here with method 1.

Method 2, as method 1, works better in an OBM well because of the same reasons as mentioned before, however, it can be used with tools that have less resolution than RXOI, like AORX and AT10. The window length has to be between 1m and 3m and the results have been positive in all OBM wells. The results in WBM wells have been quite negative, only one well (well 5) has shown something that is similar to the Triaxial Induction tool result.

Method 3 is different than 1 and 2, in that there is not relationship with the mud type and it has worked well with both types of mud. From 6 wells studied, only two of them have worked poorly, which one being with WBM and the other with OBM. This method uses the deep resistivity from AT90 or HRLT, and the purpose of the window length is only for smoothing the signal, so it is not strictly necessary. This method is based on the volume of shale calculated from the gamma ray tool, however, there are some reservoirs where the GR is not primarily due to the shale but other minerals, in these cases the method will not work. This can be seen in wells 2 and 6.

All three methods have been proved to be useful for identifying the thin laminated reservoirs in the big scale.

To summarize, if the well to be analyzed is an OBM well with a very high resolution resistivity log (a measurement each 3 cm) the best option is using method 1. If the resis-

tivity log is still a high resolution log, but with more separation between measurements (around 7cm), the best option is using method 2. If the well is drilled with WBM, the results are less reliable, but the method 3 worked well in most of them, and the result can be checked with the method 1 too, where it can be seen if a big difference between the curves exist. The important point in method 3 is that the GR responds to the real volume of shale, if not the result will be wrong.

Chapter 6

Conclusion

This work has shown that it is possible to do an estimation of Rv and Rh, and thus the resistivity anisotropy, without the necessity of a Triaxial Induction Tool. It is shown that there is not a general method that can be applied to every well, it depends on the mud type, the thickness of the mud cake, the quality of the data, the resolution of the tools and formation factors like thickness of the reservoir and natural gamma ray sources. **Fig. 6.1** summarizes which method works with which well, (**Table. 4.1** for more details about the wells), the colour green indicating a good method, the red one a bad method and the orange indicating a somewhat useful method.

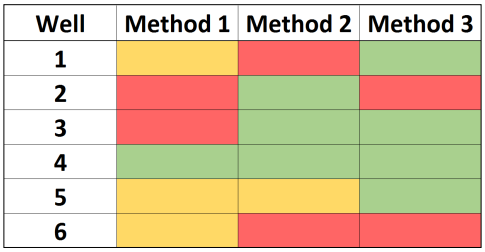

Figure 6.1: Evaluation of the methods. The colour green indicating a good method, the red one a bad method and the orange indicating a somewhat useful method.

All these methods can be very useful for the oil industry, where a big number of reservoirs are thinly laminated. The algorithms developed can be used in both, existing wells and future wells. The main use will be applying them on existing wells, where Triaxial Induction tool was not used, and the wells were declared dry or without enough volume of oil because of a low resistivity was found along the reservoir, however, this can be due to the thin laminations of shale. These algorithms can be used in these wells to identify intervals of high anisotropy indicating possible laminated shale-sand reservoirs. If the volume of oil calculated from these methods shows a significant increase, the exploration potential in that area can be reconsidered.

A secondary use of these algorithms are using them for future exploration works, where there are more than one exploration well and the use of Triaxial Induction tool is not clearly useful. The result of the algorithms in the first well can help for taking the decision of using the Triaxial Induction tool in the future wells of the same formation.

These algorithms need to be proven in more wells before using them in more important decisions, if they are successful in a significant number of wells, the use of the Triaxial Induction tool can be avoided in some areas.

Appendix A: Wells

Curve Mnemonics

GR	=	Gamma ray log.
$ECGR$	=	Environmentally Corrected Gamma Ray log.
$EHGR$	=	High Resolution Corrected Gamma Ray.
NEU	=	Thermal Neutron Porosity.
$NPHI$	=	Thermal Neutron Porosity (original Ratio Method).
$TNPH$	=	Thermal Neutron Porosity (Ratio Method).
DEN	=	Formation Density log.
$RHO8$	=	High Resolution Formation Density log.
PEF	=	Photoelectric Factor.
$HRLT$	=	High Resolution Laterolog Array Tool.
RT_HRLT	=	HRLT True Formation Resistivity.
RXO_HRLT	=	HRLT Invaded Zone Resistivity.
$RXOI$	=	Invaded Formation Resistivity Very High resolution.
$AT90$	=	Array Induction Two Foot Resistivity A90.
$AT60$	=	Array Induction Two Foot Resistivity A60.
$AT30$	=	Array Induction Two Foot Resistivity A30.
$AT20$	=	Array Induction Two Foot Resistivity A20.
$AT10$	=	Array Induction Two Foot Resistivity A10.
$ATRX$	=	Array Induction Two Foot Rxo.
$RH54\_1D$	=	Horizontal Filtered Resistivity from 54 inch Array.
$RV54\_1DF$	=	Vertical Filtered Resistivity from 54 inch Array.
$RH39\_1DF$	=	Horizontal Filtered Resistivity from 39 inch Array.
$RV39\_1DF$	=	Vertical Filtered Resistivity from 39 inch Array.
$RH39\_1DF8\_5IN\_MAINP$	=	Horizontal Filtered Resistivity from 39 inch Array.
$RV39\_1DF8\_5IN\_MAIN$	=	Vertical Filtered Resistivity from 39 inch Array.
$RH39\_1DFMAINP\_VMB$	=	Horizontal Filtered Resistivity from 39 inch Array.
$RV39\_1DFMAINP\_VMB$	=	Vertical Filtered Resistivity from 39 inch Array.
$RDEP$	=	Deep resistivity.
$RMED$	=	Medium resistivity.
$RMIC$	=	shallow resistivity.

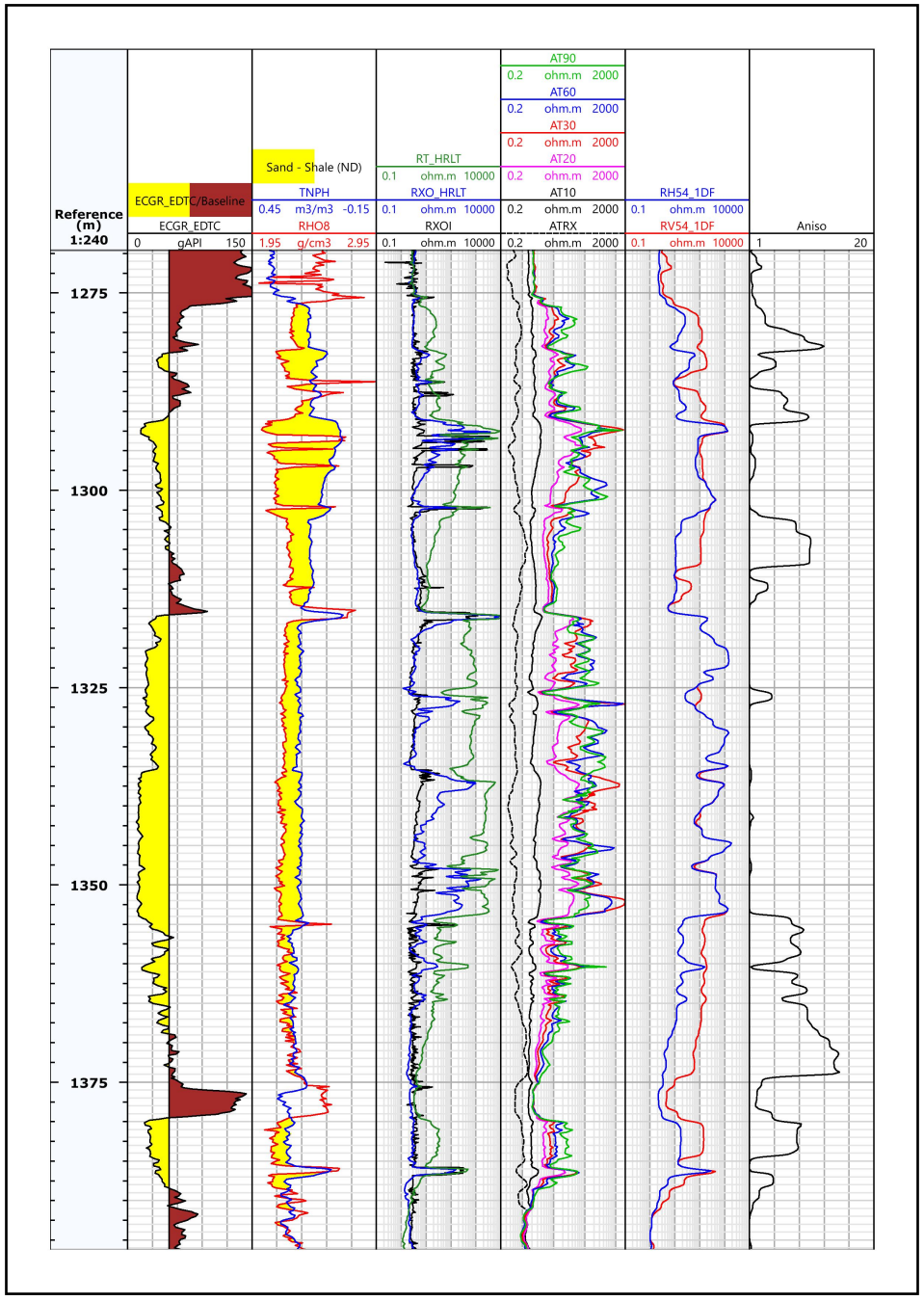

Figure 6.2: Reservoir in well 1

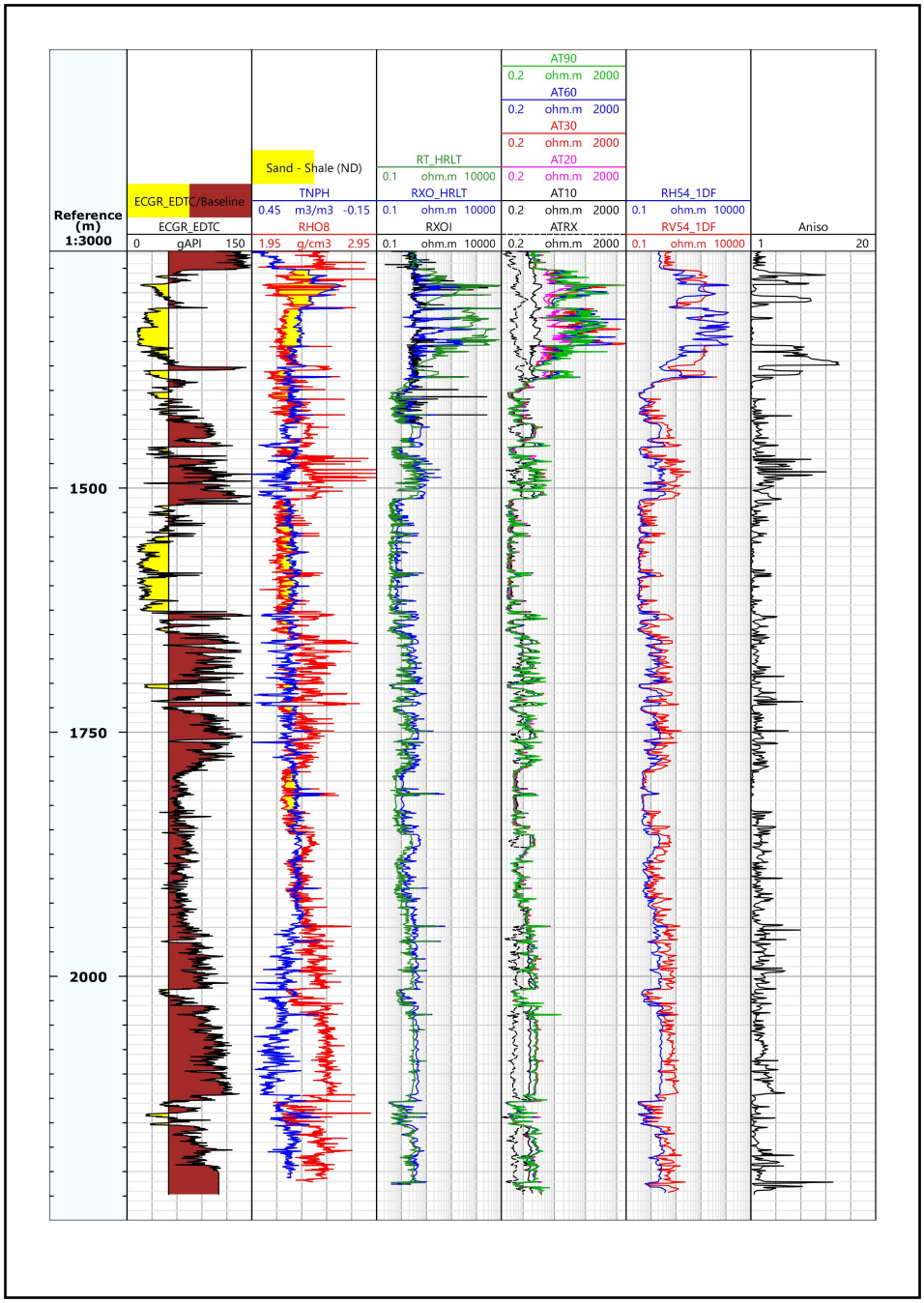

Figure 6.3: Well 1, big scale.

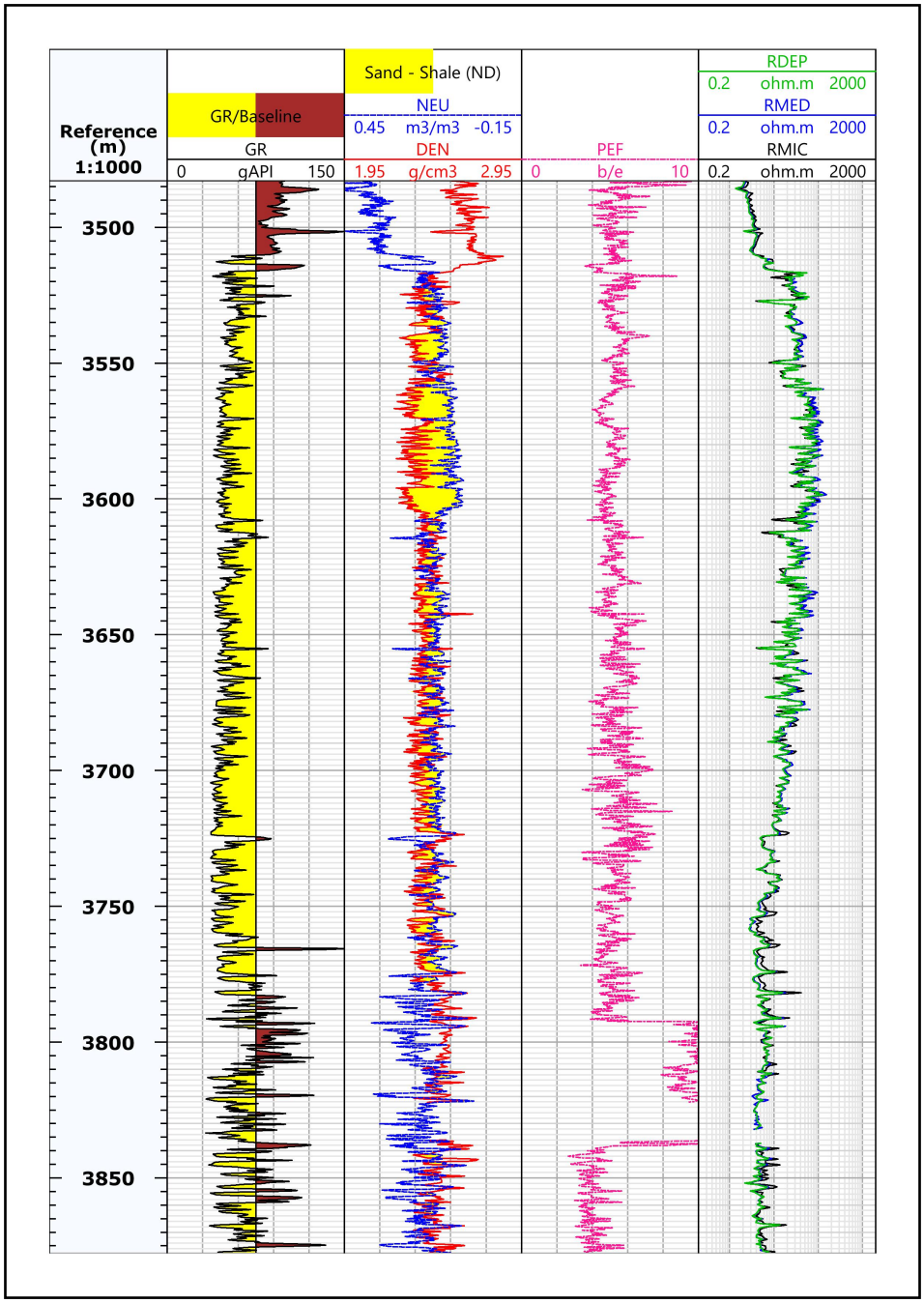

Figure 6.4: Reservoir in well 2

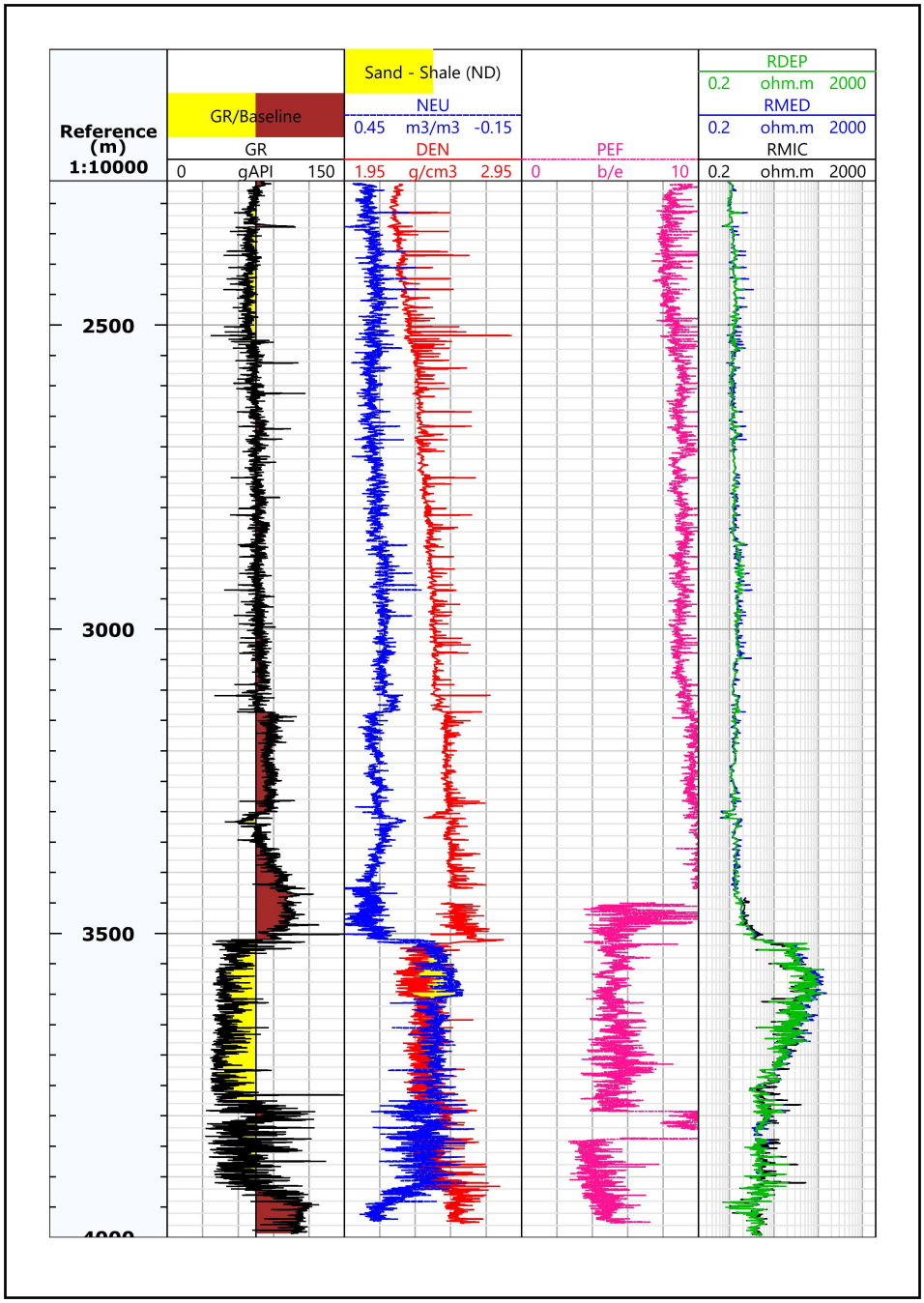

Figure 6.5: Well 2, big scale.

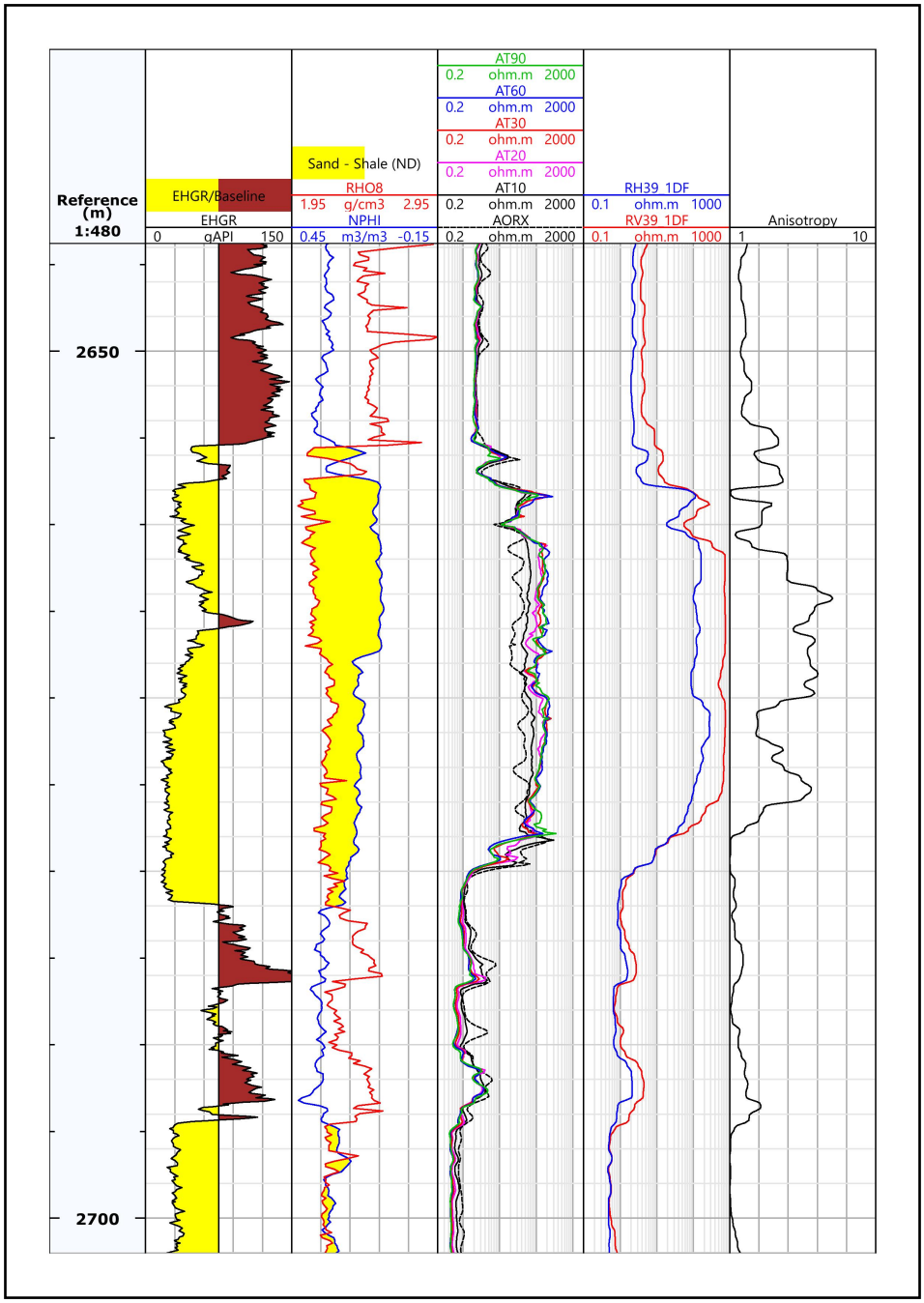

Figure 6.6: Reservoir in well 3

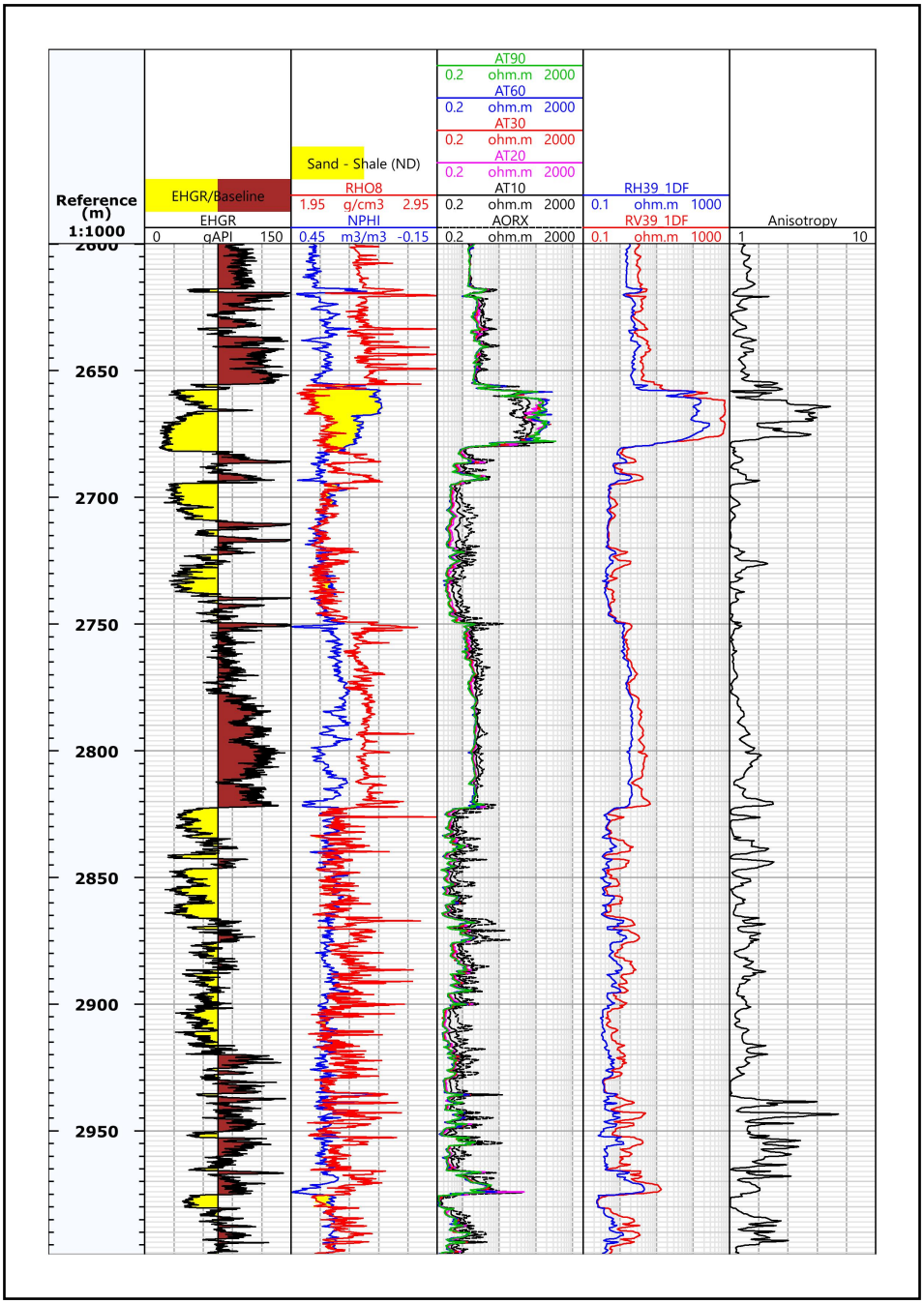

Figure 6.7: Well 3, big scale.

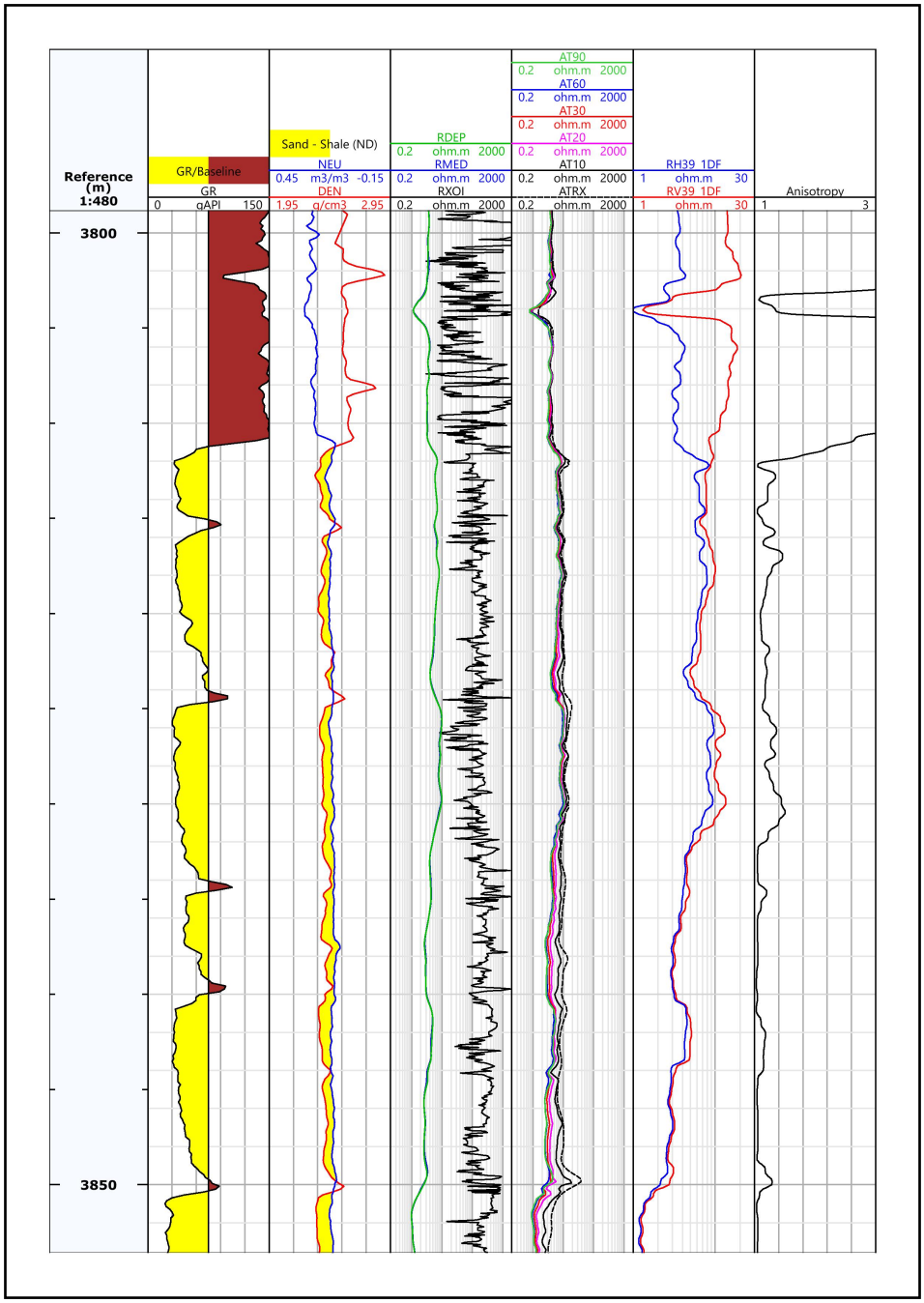

Figure 6.8: Reservoir in well 4

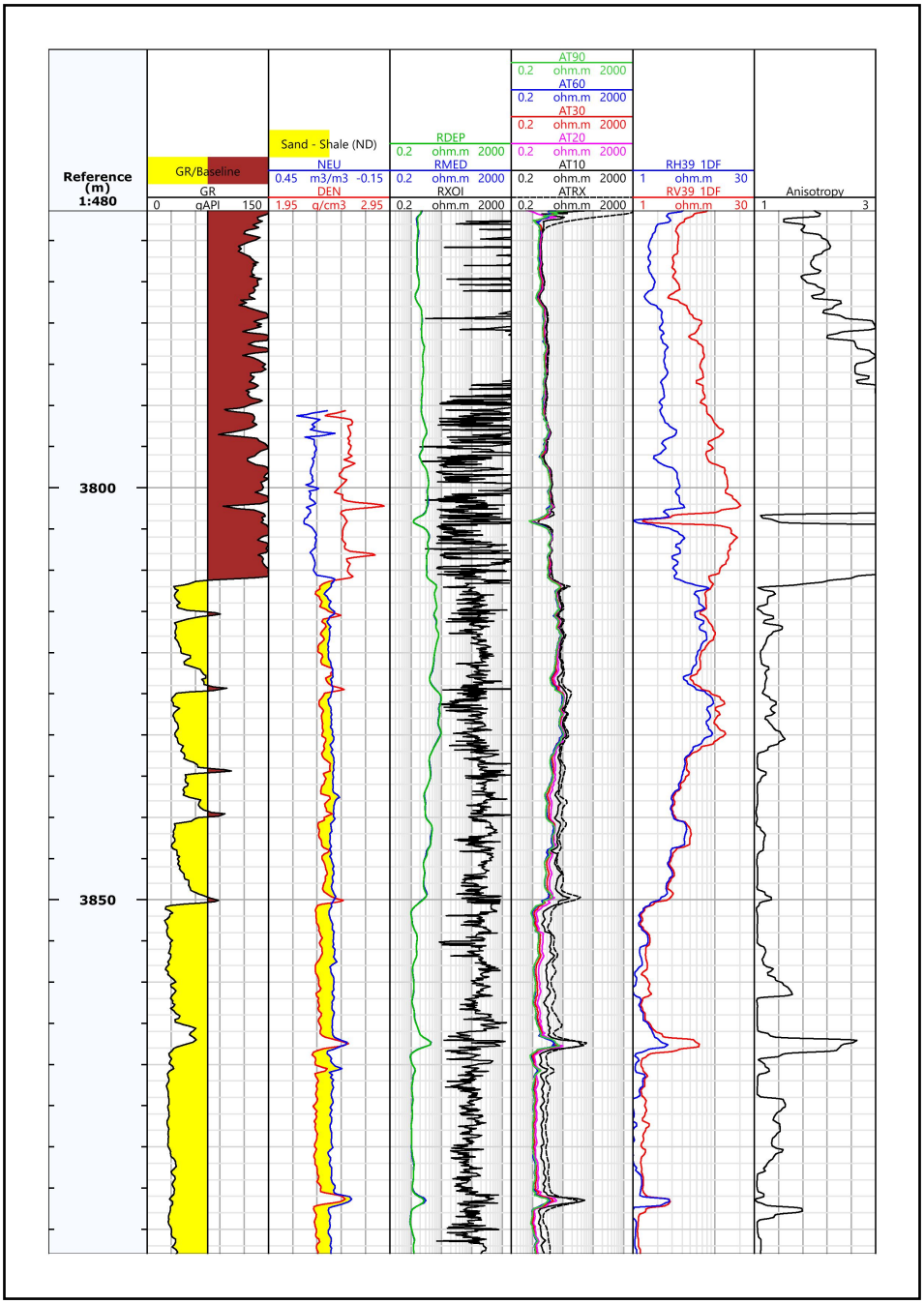

Figure 6.9: Well 4, big scale.

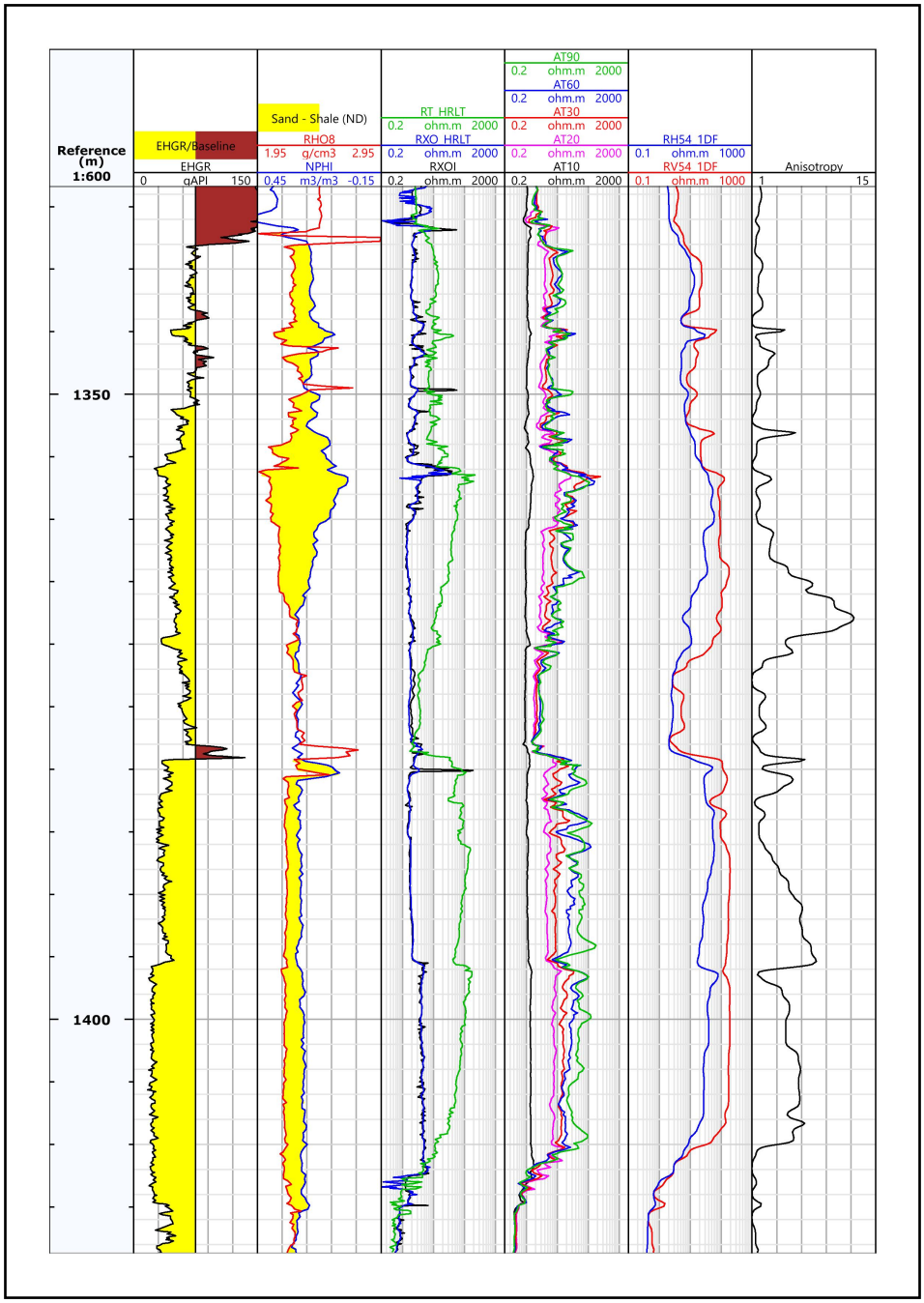

Figure 6.10: Reservoir in well 5

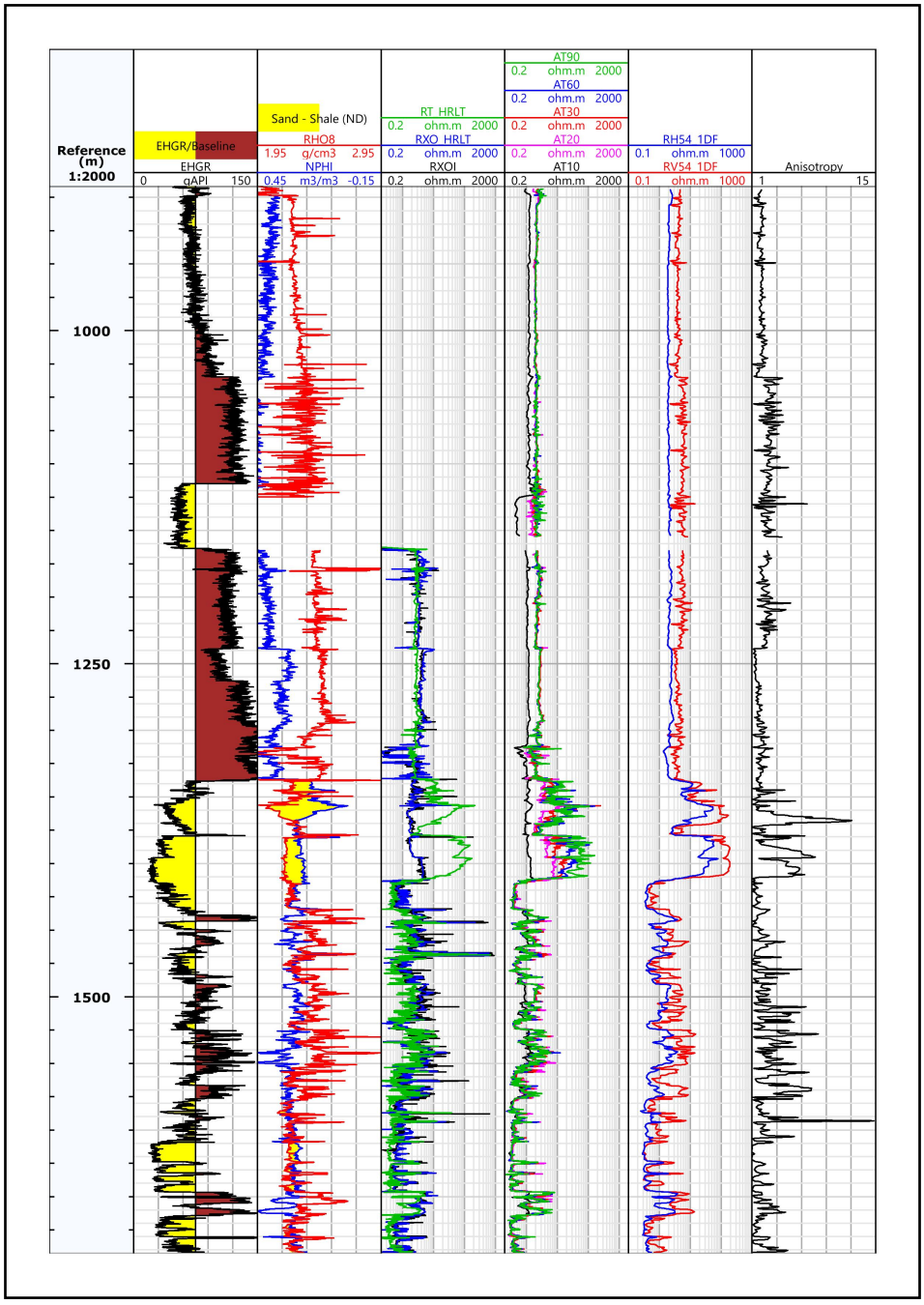

Figure 6.11: Well 5, big scale.

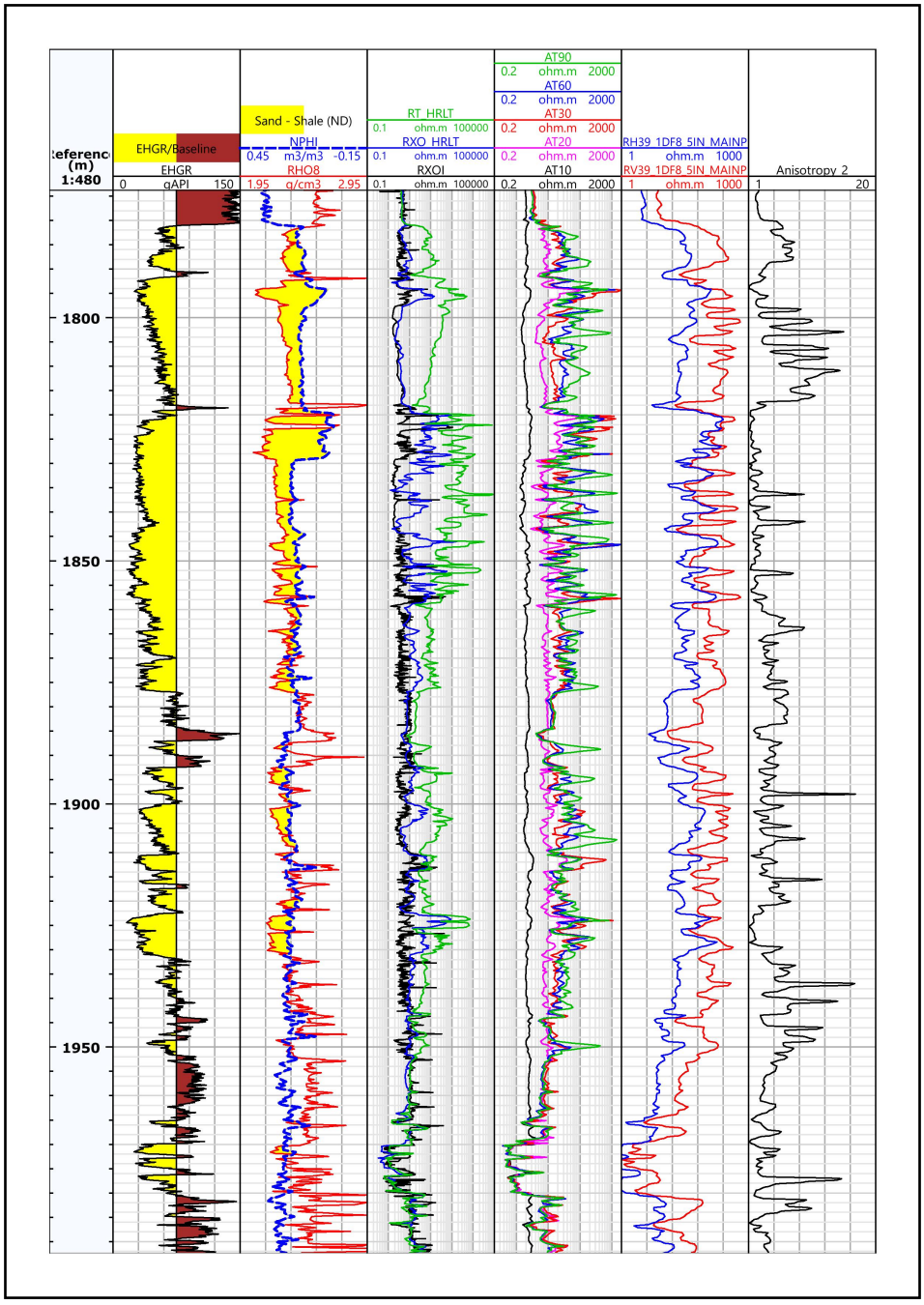

Figure 6.12: Reservoir in well 6

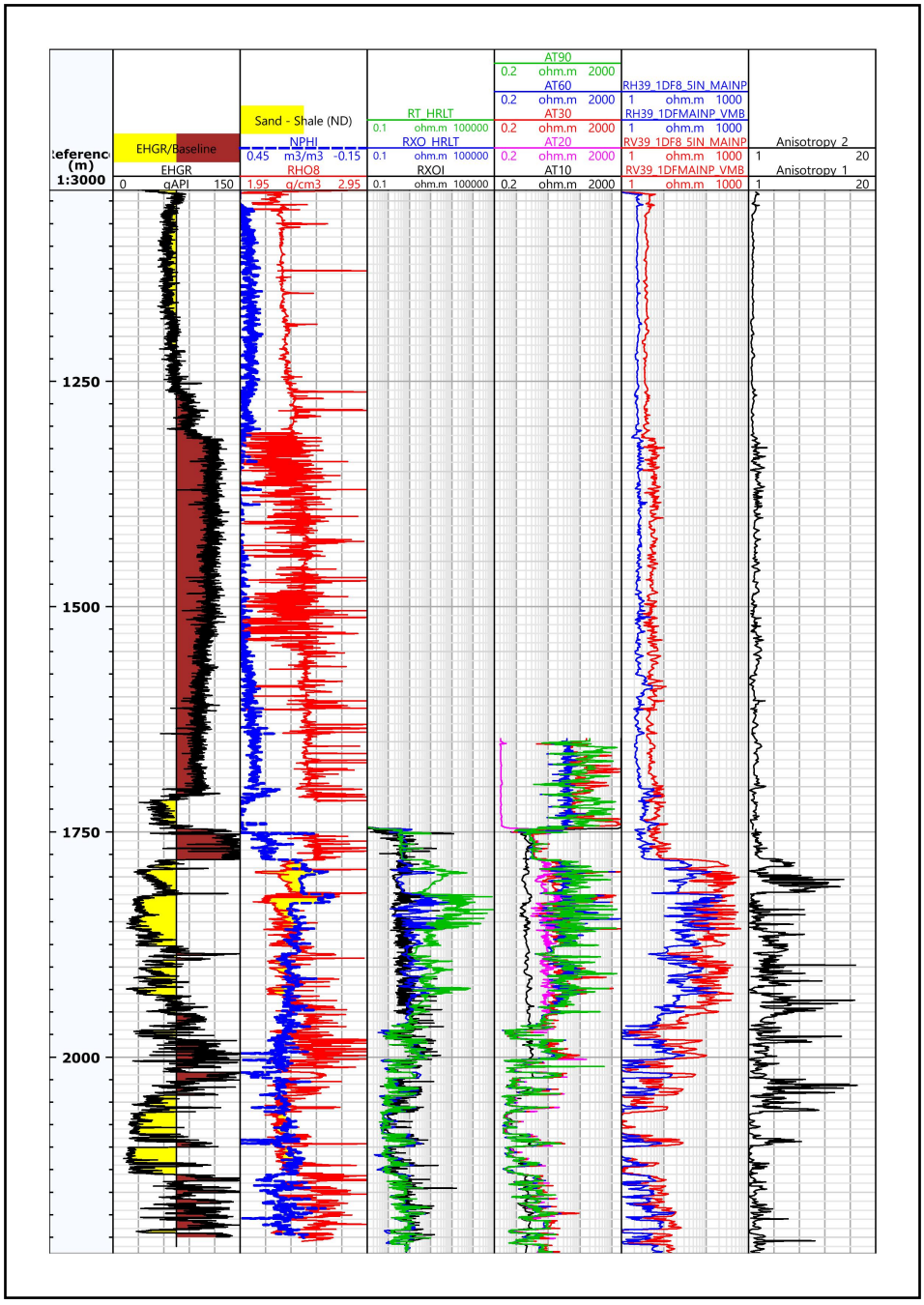

Figure 6.13: Well 6, big scale.

Appendix B: Code

Method 1: estimating Rv from a convolution average filter.

```
%Method 1: estimating Rv from a convolution average filter.

Depth = xlsread('Resistivity.xlsx', 1); %Input depths of the resistivity
    measures.
R1 = xlsread('Resistivity.xlsx', 2); %Input the resistivity measures.
m1 = size(Depth);
n1 = m1(1, 1); %Total number of measures.
h = input('Window length: ');
f = floor(h/2) + 1; %Half of the window length (natural number).

%We define a vector R2 (size of n1+2*f) from R1 (size of n1) for being
%able to apply a convolution filter. We have to set "f" values in the
%beginnig and "f" values in the end of the vector, these values are chosen
%to be the first and the last value of the R1 vector.
R2 = zeros((n1 + 2*f), 1);
for i = 1:(n1 + 2*f)
    if i <= f;
       R2(i, 1) = R1(1, 1);
    elseif i >= (n1 + f);
       R2(i, 1) = R1(n1, 1);
    else
       R2(i, 1) = R1((i - f), 1);
    end
end

%Convolution filter applied over R2 for computing Rv, Rh and A. This has
%been applied for two cases, the first one is in the case that we window
%length is even, and the second one if the window length is odd.
Rv = zeros(n1, 1);
Rh = zeros(n1, 1);
A = zeros(n1, 1);
for i = (f + 1):(n1 + f)
    if rem(h, 2) == 0;
       a1 = 0;
       sum1 = 0;
       sum3 = 0;
          for j = (i - (h/2)):(i + (h/2));
            a1 = R2(j, 1);
            sum1 = sum1 + a1;
            sum3 = sum3 + (1/a1);
          end
       Rv((i-f), 1) = sum1/(h + 1);
       Rh((i-f), 1) = ((h + 1)/sum3);
       A((i-f), 1) = Rv((i - f), 1)/Rh((i - f), 1);
    else
```

```
45          a2 = 0;
46          sum2 = 0;
47          sum3 = 0;
48             for j = (i - ((h - 1)/2)):(i + ((h - 1)/2));
49               a2 = R2(j, 1);
50               sum2 = sum2 + a2;
51               sum3 = sum3 + (1/a2);
52              end
53          Rv((i-f), 1) = sum2/h;
54          Rh((i-f), 1) = (h/sum3);
55          A((i-f), 1) = Rv((i - f), 1)/Rh((i - f), 1);
56      end
57  end
58
59  %input of Rv and Rh measured by Triaxial induction tool.
60  deptho = xlsread('Anisotropy.xlsx', 1); %Input depths of the resistivity
        measures.
61  Rvo = xlsread('Anisotropy.xlsx', 2); %Input the vertical resistivity
        measures.
62  Rho = xlsread('Anisotropy.xlsx', 3); %Input the horizontal resistivity
        measures.
63  Ao = xlsread('Anisotropy.xlsx', 4); %Input the anisotropy.
64
65  %interpolation for having the same number of points, and having each
66  %measure in the same depth for being able to use plot.
67  Rvm = interp1(deptho, Rvo, Depth);
68  Rhm = interp1(deptho, Rho, Depth);
69  Am = interp1(deptho, Ao, Depth);
70
71  %Plot for comparing Rv and Rh estimated with the convolution filter, with
72  %Rv and Rh measured by triaxial induction tool.
73  semilogy(Depth, Rvm, Depth, Rhm, Depth, Rv, Depth, Rh);
74  legend('Rv measured', 'Rh measured', 'Rv estimated', 'Rh estimated')
75
76  %Plot for comparing the Anisotropy estimated with the convolution filter,
77  %with the anisotropy measured by Triaxial induction tool.
78  plot(Depth, Am, Depth, A)
79  legend('A measured','A estimated')
```

Method 2: estimating Rv from the estimation of the resistivity of the sand.

```
%Method 2: estimating Rv from the estimation of the resistivity of the
    sand.

Depth = xlsread('Resistivity.xlsx', 1); %Input depths of the resistivity
    measures.
R1 = xlsread('Resistivity.xlsx', 2); %Input the resistivity measures.
m1 = size(Depth);
n1 = m1(1, 1); %Total number of measures.
h = input('Window length: ');

%This will create a square function "R", with the maximum values of the
%resistivity along the windows that has been defined. This is considered
%the resistivity of the sand.
%"w" is the number of windows where the maximum value of resistivity is
%going to be looked fore.
w = floor(n1/h);
R = zeros(n1, 1);
for j = 1:(w - 1);
    if j == 1
       z = zeros(n1, 1);
          for i = j:(j + h - 1)
            z(i, 1) = R1(i, 1);
          end
       M = max(z);

          for i = j:(j + h - 1)
            R((j + i - 1), 1) = M;
          end
    end
    if j ~= 1
       z = zeros(n1, 1);
          for i = ((j - 1)*h + 1):(((j - 1)*h + 1) + h - 1)
            z(i, 1) = R1(i, 1);
          end
       M = max(z);

          for i = ((j - 1)*h + 1):(((j - 1)*h + 1) + h - 1)
            R(i, 1) = M;
          end
    end
end

%This will create a vector with the length of "R1" and the resistivity of
%the shale in all the components.
sh = input('Resistivity of the shale: ');
r = ones(n1, 1)*sh;

%Input gammaray and Triaxial Induction tool measures.
deptho = xlsread('GammaRay.xlsx', 1); %Input depths of the GR measures.
Gamma = xlsread('GammaRay.xlsx', 2); %Input the GR measures.
deptht = xlsread('Anisotropy.xlsx', 1); %Input depths of the anisotropy.
Rvo = xlsread('Anisotropy.xlsx', 2); %Input the vertical resistivity
    measures.
```

```
Rho = xlsread('Anisotropy.xlsx', 3); %Input the horizontal resistivity
    measures.
Ao = xlsread('Anisotropy.xlsx', 4); %Input the anisotropy.

%Computing the maximum and minimum of the Gamma Ray log.
GM = max(Gamma);
Gm = min(Gamma);

%Interpolation for having the same number of points, and having each
%measure in the same depth for being able to make operations between them.
GRm = interp1(deptho, Gamma, Depth);
Am = interp1(deptht, Ao, Depth);
Rvm = interp1(deptht, Rvo, Depth);
Rhm = interp1(deptht, Rho, Depth);

%Calculus of the volume of shale and sand.
Vshale = zeros(n1, 1);
Vsand = zeros(n1, 1);
for i = 1:n1
    Vshale(i, 1) = (GRm(i, 1) - Gm)/(GM - Gm);
    Vsand(i, 1) = (1 - Vshale(i, 1));
end

%calculus of Rh and Rv.
Rv = zeros(n1, 1);
Rh = zeros(n1, 1);
A = zeros(n1, 1);
for i=1:n1
    Rv(i, 1) = Vsand(i, 1)*R(i, 1) + Vshale(i, 1)*r(i, 1);
    Rh(i, 1) = (1/((Vsand(i, 1)/R(i, 1)) + (Vshale(i, 1)/r(i, 1))));
    A(i, 1) = Rv(i, 1)/Rh(i, 1);
end

%Plot for comparing Rv and Rh estimated with this method, with
%Rv and Rh measured by triaxial induction tool.
semilogy(Depth, Rvm, Depth, Rhm, Depth, Rv, Depth, Rh);
legend('Rv measured', 'Rh measured', 'Rv estimated', 'Rh estimated')

%Plot for comparing the Anisotropy estimated with this method,
%with the anisotropy measured by Triaxial induction tool.
plot(Depth, Am, Depth, A)
legend('A measured', 'A estimated')
```

Method 3: estimating Rv from the deep resistivity and GR tool.

```
%Method 3: estimating Rv from the deep resistivity and GR tool.

Depth = xlsread('Resistivity.xlsx', 1); %Input depths of the resistivity
    measures.
R1 = xlsread('Resistivity.xlsx', 2); %Input the resistivity measures.
m1 = size(Depth);
n1 = m1(1, 1); %Total number of measures.

%Input gammaray and Triaxial Induction tool measures.
deptht = xlsread('GammaRay.xlsx', 1); %Input depths of the GR measures.
GR = xlsread('GammaRay.xlsx', 2); %Input the GR measures.
deptho = xlsread('Anisotropy.xlsx', 1); %Input depths of the anisotropy.
Rvo = xlsread('Anisotropy.xlsx', 2); %Input the vertical resistivity
    measures.
Rho = xlsread('Anisotropy.xlsx', 3); %Input the horizontal resistivity
    measures.
Ao = xlsread('Anisotropy.xlsx', 4); %Input the anisotropy.

%Computing the maximum and minimum of the Gamma Ray log.
GM = max(GR);
Gm = min(GR);

%Interpolation for having the same number of points, and having each
%measure in the same depth for being able to make operations between them.
GRm = interp1(deptht, GR, Depth);
Rvm = interp1(deptho, Rvo, Depth);
Rhm = interp1(deptho, Rho, Depth);
Am = interp1(deptho, Ao, Depth);

%Calculus of the volume of shale and sand.
Vshale = zeros(n1, 1);
Vsand = zeros(n1, 1);
for i = 1:n1
    Vshale(i, 1) = (GRm(i, 1) - Gm)/(GM - Gm);
    Vsand(i, 1) = (1 - Vshale(i, 1));
end

Rshale = input('Resistivity of the shale: ');

%This will compute the resistivity of the sand, doing the estimation that
%"R1" is the horizontal resistivity. Knowing "Rsand", "Rv" can be computed
    .
Rsand = zeros(n1, 1);
Rv1 = zeros(n1, 1);
for i = 1:n1
    Rsand(i,1) = Vsand(i, 1)/(1/R1(i, 1) - Vshale(i, 1)/Rshale);
    Rsand2 = abs(Rsand);
    Rv1(i,1) = Vsand(i, 1)*Rsand2(i, 1) + Vshale(i, 1)*Rshale;
end

h = input('Window length for smoothing the signal:');
u = ones(h, 1);
Rv2 = conv(Rv1, u)/h;
```

```
Rh2 = conv(R1, u)/h;

%This will cut the vectors "Rv2" and "Rh2" for having the same size that
%the rest of the signal and being able to compare them.
Rv = zeros(n1, 1);
for i = 1:n1
    Rv(i, 1) = Rv2((i + floor(h/2)), 1);
end
Rh = zeros(n1, 1);
for i=1:n1
    Rh(i, 1) = Rh2((i + floor(h/2)), 1);
end

%This will compute the anisotropy, giving the value of "1" if the
%anisotropy calculated is less than 1.
A = zeros(n1, 1);
for i = 1:n1
    A(i, 1) = Rv(i, 1)/Rh(i, 1);
    if A(i, 1) < 1
        A(i, 1) = 1;
    end
end

%Plot for comparing Rv and Rh estimated with this method, with
%Rv and Rh measured by triaxial induction tool.
semilogy(Depth, Rvm, Depth, Rhm, Depth, Rv, Depth, Rh);
legend('Rv measured', 'Rh measured', 'Rv estimated', 'Rh estimated')

%Plot for comparing the Anisotropy estimated with this method,
%with the anisotropy measured by Triaxial induction tool.
plot(Depth, Am, Depth, A)
legend('A measured', 'A estimated')
```

Bibliography

Allen, D. F., et al., 1984. Laminated sand analysis. In: SPWLA 25th Annual Logging Symposium. Society of Petrophysicists and Well-Log Analysts.

Anderson, B., Barber, T., Leveridge, R., Bastia, R., Saxena, K. R., Tyagi, A. K., Clavaud, J.-B., Coffin, B., Das, M., Hayden, R., et al., 2008. Triaxial induction. a new angle for an old measurement. Analyst 23 (1), 20–34.

Anderson, B., Bryant, I., Luling, M., Spies, B., Helbig, K., 1994. Oil-field anisotropy-its origins and electrical characteristics. Oilfield Review 6 (4), 48–56.

Anderson, B. I., Barber, T. D., et al., 1988. Using computer modeling to provide missing information for interpreting resistivity logs. In: SPWLA 29th Annual Logging Symposium. Society of Petrophysicists and Well-Log Analysts.

Bateman, R. M., 1990. Thinbed analysis with conventional log suites.

Clavaud, J.-B., Nelson, R., Guru, U. K., et al., 2005. Field example of enhanced hydrocarbon estimation in thinly laminated formation with a triaxial array induction tool: A laminated sand-shale analysis with anisotropic shale. In: SPWLA 46th Annual Logging Symposium. Society of Petrophysicists and Well-Log Analysts.

Engelmark, F., Mattsson, J., 2013. Estimating vertical and horizontal resistivity of the overburden and the reservoir for the alvheim–boa field. In: SEG Technical Program Expanded Abstracts 2013. Society of Exploration Geophysicists, pp. 856–860.

Faivre, O., Barber, T., Jammes, L., Vuhoang, D., et al., 2002. Using array induction and array laterolog data to characterize resistivity anisotropy in vertical wells. In: SPWLA 43rd Annual Logging Symposium. Society of Petrophysicists and Well-Log Analysts.

Hagiwara, T., et al., 1995. Induction log analysis of thinly laminated sand/shale formation. SPE Formation Evaluation 10 (02), 86–90.

Hossain, Z., Newton*, P. V. d., 2014. Vertical and horizontal resistivity analysis by an electrical anisotropy template. In: SEG Technical Program Expanded Abstracts 2014. Society of Exploration Geophysicists, pp. 2439–2443.

Klein, J. D., Martin, P., et al., 1997. The petrophysics of electrically anisotropic reservoirs. The Log Analyst 38 (03).

Liu, Z., Torres-Verdín, C., Wang, G. L., Mendoza, A., Zhu, P., Terry, R., et al., 2007. Joint inversion of density and resistivity logs for the improved petrophysical assessment of thinly-bedded clastic rock formations. In: 48th Annual Logging Symposium. Society of Petrophysicists and Well-Log Analysts.

Minh, C. C., Clavaud, J.-B., Sundararaman, P., Froment, S., Caroli, E., Billon, O., Davis, G., Fairbairn, R., et al., 2008. Graphical analysis of laminated sand-shale formations in the presence of anisotropic shales1. Petrophysics 49 (05).

Oshnyakov, I., Khabarov, A., Malshakov, A., et al., 2014. Evaluation of thin laminated reservoirs-hidden problems. In: SPE Russian Oil and Gas Exploration & Production Technical Conference and Exhibition. Society of Petroleum Engineers.

Passey, Q., Dahlberg, K., Sullivan, K., Yin, H., Xiao, Y., Guzman-Garcia, A., Brackett, R., et al., 2004. A systematic approach to evaluate hydrocarbons in thinly bedded reservoirs. In: SPWLA 45th Annual Logging Symposium. Society of Petrophysicists and Well-Log Analysts.

Pavlovic, M., Rabinovich, M., Tabarovsky, L., Corley, B., Munkholm, M., et al., 2002. Integrated resistivity interpretation of array induction, multi-component induction and borehole resistivity imaging measurements in thinly bedded sand-shale sequences. In: SPWLA 43rd Annual Logging Symposium. Society of Petrophysicists and Well-Log Analysts.

Sanchez-Ramirez, J. A., Torres-Verdín, C., Wang, G. L., Mendoza, A., Wolf, D., Liu, Z., Schell, G., et al., 2009. Field examples of the combined petrophysical inversion of gamma-ray, density, and resistivity logs acquired in thinly-bedded clastic rock formations. In: SPWLA 50th Annual Logging Symposium. Society of Petrophysicists and Well-Log Analysts.

Tabanou, J. R., Cheung, P., Liu, C. B., Hansen, S., Lavigne, J., Pickens, T., Borbas, T., Wendt, B., et al., 2002. Thinly laminated reservoir evaluation in oil-base mud: High resolution versus bulk anisotropy measurement-a comprehensive evaluation. In: SPWLA 43rd Annual Logging Symposium. Society of Petrophysicists and Well-Log Analysts.

van den Berg, F. G., Looyestijn, W. J., Sandor, R. K., et al., 1996. Sandwich: Log evaluation in laminated shaly sands. In: SPWLA 37th Annual Logging Symposium. Society of Petrophysicists and Well-Log Analysts.

Woodhouse, R., Greet, D. N., Mohundro, C., et al., 1984. Induction log vertical resolution improvement in vertical and deviated wells using a practical deconvolution filter. Journal of petroleum technology 36 (06), 993–1.